# Decarbonizing global power supply under region-specific consideration of challenges and options of integrating variable renewables in the REMIND model

Falko Ueckerdt[#]*, Robert Pietzcker[#]*, Yvonne Scholz[+], Daniel Stetter[+], Anastasis Giannousakis[#], Gunnar Luderer[#]

[#] *Potsdam Institute for Climate Impact Research (PIK), PO Box 601203, 14412 Potsdam, Germany*

[+] *German Aerospace Center (DLR) Stuttgart, Pfaffenwaldring 38-40, 70569 Stuttgart, Germany*

**Corresponding authors E-mail: ueckerdt@pik-potsdam.de, pietzcker@pik-potsdam.de, F. Ueckerdt and R.C. Pietzcker contributed equally to this work*

We present two advances in representing variable renewables (VRE) in global energy-economy-climate models: accounting for region-specific integration challenges for eight world regions and considering short-term storage. Both advances refine the approach of implementing residual load duration curves (RLDCs) to capture integration challenges. In this paper we derive RLDCs for eight world regions (based on region-specific time series for load, wind and solar) and implement them into the REMIND model. Therein we parameterize the impact of short-term storage using the highly-resolved model DIMES. All RLDCs and the underlying region-specific VRE time series are made available to the research community. We find that the more accurate accounting of integration challenges in REMIND does not reduce the prominent role of wind and solar in scenarios that cost-efficiently achieve the 2°C target. Until 2030, VRE shares increase to about 15-40% in most regions with limited deployment of short-term storage capacities (below 2% of peak load). The REMIND model's default assumption of large-scale transmission grid expansion allows smoothening variability such that VRE capacity credits are moderate and curtailment is low. In the long run, VRE become the backbone of electricity supply and provide more than 70% of global electricity demand from 2070 on. Integration options ease this transformation: storage on diurnal and seasonal scales (via flow batteries and hydrogen electrolysis) and a shift in the non-VRE capacity mix from baseload towards more peaking power plants. The refined RLDC approach allows for a more accurate consideration of system-level impacts of VRE, and hence more robust insights on the nature of power sector decarbonization and related economic impacts.

# 1. Introduction

Future power systems will likely show a significant share of renewable energy of which a large contribution will come from the *variable*[1] renewable energy sources (VRE): wind and solar photovoltaics (PV). This is indicated by current high annual growth rates (end-2009 through 2014: 19% for wind capacity and 50% for solar PV capacity, [1]) as well as renewable support schemes and ambitious policy targets (164 countries had defined renewable targets by early 2015).

Global energy-economy-climate models for cost-optimal climate mitigation scenarios typically also show a prominent role of VRE for low-carbon power supply [2]–[8]. However, the inability of these models to explicitly represent the time-scales relevant for the short-term variability of VRE supply and electricity demand limits their ability to capture the challenges and options of integrating VRE. Recent studies based on detailed power market models have shown that integration costs, or the decreasing impact of variability on the economic value of VRE generation, can be as high as long-term projection of VRE generation costs [9]–[14], suggesting that the bias from an inaccurate representation of variability may be large. As VRE generation costs decrease below those of conventional generation, in particular with increasing $CO_2$ prices, integration challenges increasingly become the key determinant of the role of VRE generation in future low-carbon power systems. Hence, accounting accurately for VRE integration is a prerequisite for deriving robust mitigation scenarios, estimating economic impacts of climate policies and determining the specific role of VRE.

Over the last years, significant efforts were made by modellers of the long-term evolution of the energy-economy-climate system to address this important shortcoming. Different modelling approaches for representing variability were developed (see overviews in [7], [15]). The so-called RLDC approach was introduced and applied to a REMIND version for the German energy system and economy in [15] and further refined and applied to the European region in the MERGE model in [16]. Its core is a model implementation of residual load duration curves (RLDCs) that change endogenously with wind and solar PV deployment. These curves capture the temporal matching of VRE supply with load, and thereby capture the drivers of so-called "profile costs", which account for the dominant share of VRE integration costs [10], [13], [17]. While profile costs can even be negative at low shares, e.g., for solar PV in many US regions, profile costs are the largest cost impact imposed by VRE variability at higher shares of VRE[2], i.e., they tend to be substantially larger than costs related to additional balancing or grid requirements of VRE. Profile costs encompass three major effects: a low capacity credit and resulting requirements for firm capacity, reduced utilization of the capital embodied in dispatchable plants[3], and over-produced[4] VRE generation. All these three effects are captured by RLDCs [10], [17]. RLDCs hereby also account for

[1] "Variable" (or sometimes intermittent) is used to describe generators that rely on fluctuating weather conditions (wind and solar plants) and thus can hardly be controlled in their power output.

[2] The reason is that the supply of additional VRE plants is correlated with the existing VRE plants and thus the matching with residual demand gets unfavorable at higher VRE shares.

[3] In principle, the utilization is reduced for all dispatchable plants; however, for capital-intensive base-load plants this is particularly costly.

[4] Over-produced VRE generation exceeds electricity demand and cannot directly be used. It needs to be curtailed if it cannot be used as an alternative input e.g. for electricity storage.

the diminishing marginal value of additional VRE generators due to correlation with existing VRE generation [11], [13].

This paper presents two key refinements of the RLDC approach: a region-specific representation of integration challenges for several world regions and a sophisticated representation of storage parameterized by the highly-resolved **D**ispatch and **I**nvestment **M**odel for **E**lectricity **S**torage (DIMES) model, which optimizes investments and dispatch of power plants and storage technologies based on an hourly temporal resolution.

1) Integration challenges can significantly differ around the world, in particular at VRE shares of up to about 30% [17]. We apply the RLDC approach for the first time to more than one region. It is parameterized from data for eight world regions and implemented for eleven[5] regions of the global energy-economy-climate model REMIND. This requires a region-specific parameterization of RLDCs based on global time series data for VRE supply and load. Highly resolved load data is hardly available for most developing and emerging economies and it has been a major effort to collect a range of time series. To foster adoption of the methodology by other modellers, all RLDCs that have been derived to parameterize REMIND and the underlying VRE supply time series are available in the supplementary materials to this paper.
2) The second key refinement of the RLDC approach is a sophisticated representation of short-term storage, which is based on a parameterization by a large set of model runs[6] conducted by the highly-resolved DIMES model. Our results indicate that without a representation of storage operating on diurnal time scales, the potential of solar PV tends to be underestimated. In addition, the approach contains an endogenous representation of long-term storage via hydrogen electrolysis, which was also employed in [15], [16].

The resulting model representation of variability differentiates between a broad range of wind and solar PV shares, a number of world regions and accounts for potentially important integration options such as storage, transmission grid costs for large area pooling (which is a default assumption in REMIND), and the adaptation of the non-VRE generation capacities in response to VRE deployment. Based on the methodological advances, mitigation scenario results become more robust and thus more relevant for policy advice.

The paper is structured as follows. We introduce the method in section 2 and present results in section 3. In a first results section (3.1) we illustrate based on RLDCs how integration challenges differ (and do not differ) between regions, VRE mixes and shares. We also discuss the impact of short-term storage on RLDCs. In a second results section (3.2) we relate REMIND scenario results based on the implemented RLDCs to the region-specific integration challenges. In the presentation of the results we focus on the three regions Europe, USA and Sub-Saharan Africa because they show an instructive range of integration challenges.

[5] Three REMIND model regions have no individual parameterization due to a lack of load data. They are approximated by the representations of related model regions.
[6] 1352 DIMES model runs result from parameterizing 8 regions for gross wind and solar shares each ranging from 0% to 120% (in 10% steps).

This paper is part of a special section in this Energy Economics issue on system integration challenges of VRE and the representation of these challenges in global energy-economy-climate models, resulting from the ADVANCE project. For a detailed comparison of the REMIND RLDC representation of system integration challenges with other modelling approaches in other IAMs, see [18] (this issue). The relative importance of costs, resource potentials and integration challenges for VRE deployment in REMIND and the other contributing IAMs is analyzed in [19] (this issue).

## 2. Method

This section is structured as follows. We briefly describe the REMIND model in section 2.1 and the scenario definitions in section 2.2. In the following subsections we present the three key methodical steps that have been conducted to improve the REMIND model (illustrated in Figure 1). First, we collected global load and VRE supply time series data, which we spatially aggregated according to the REMIND model regions (section 2.3). Second, we fed the data into the highly-resolved model DIMES to derive a comprehensive set of RLDCs (for a range of exogenous gross[7] VRE shares and mixes) that include the impact of short-term storage (section 2.4). Third, we implemented the region-specific RLDCs into the REMIND model as approximate step functions that change endogenously with VRE mix and share (section 2.5). Section 2.6 offers a discussion of limitations of the method used and potential for further refinements (section 2.6).

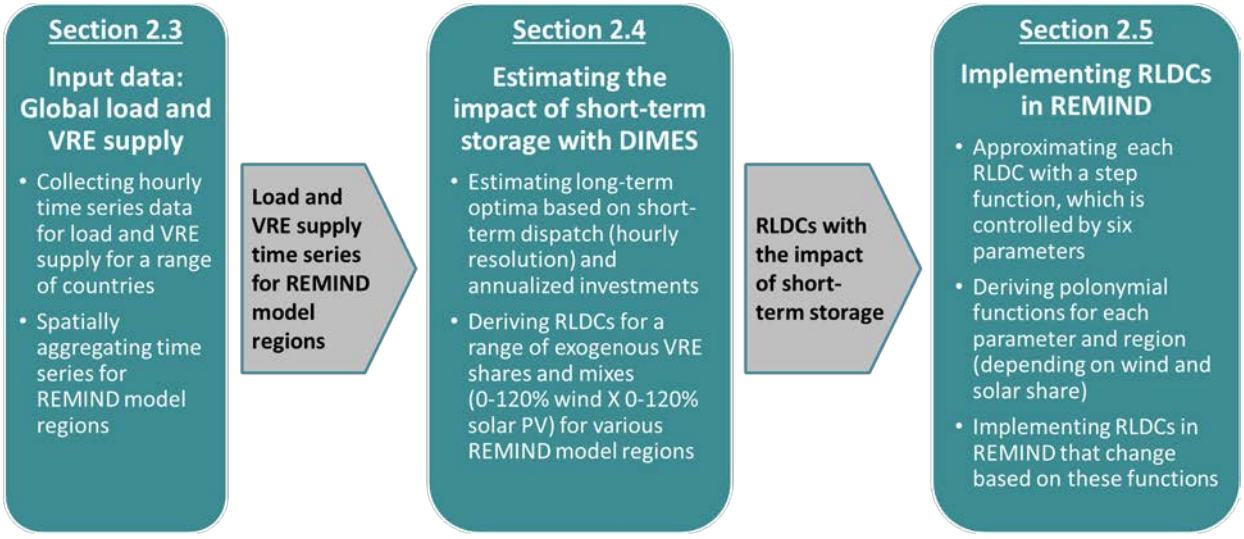


**Figure 1 : The three key methodical steps comprise i) collecting global load and VRE supply data, ii) estimating the impact of short-term storage and iii) implementing region-specific RLDCs into the REMIND model.**

### 2.1. REMIND model

This is a brief description. A more elaborate description can be found in the published model documentation [20]. See also applications in Ref. [21]–[23]. The energy-economy-climate model REMIND is a Ramsey-type general equilibrium growth model of the macro-economy in which inter-

[7] « Gross » share refers to the ratio of potential annual VRE generation (i.e. including curtailment) and total annual load.

temporal global welfare is maximized, combined with a technology-rich representation of the energy system. It represents capacity stocks of more than 50 conventional and low-carbon energy conversion technologies, including 20 different renewable and non-renewable electricity generation technologies. REMIND accounts for relevant path-dependencies, such as the build-up of long-lived capital stocks, as well as learning-by-doing effects and inertias in the up-scaling of innovative technologies. REMIND operates in time-steps of five years for the period from 2005 to 2060, and ten years for the rest of the century.

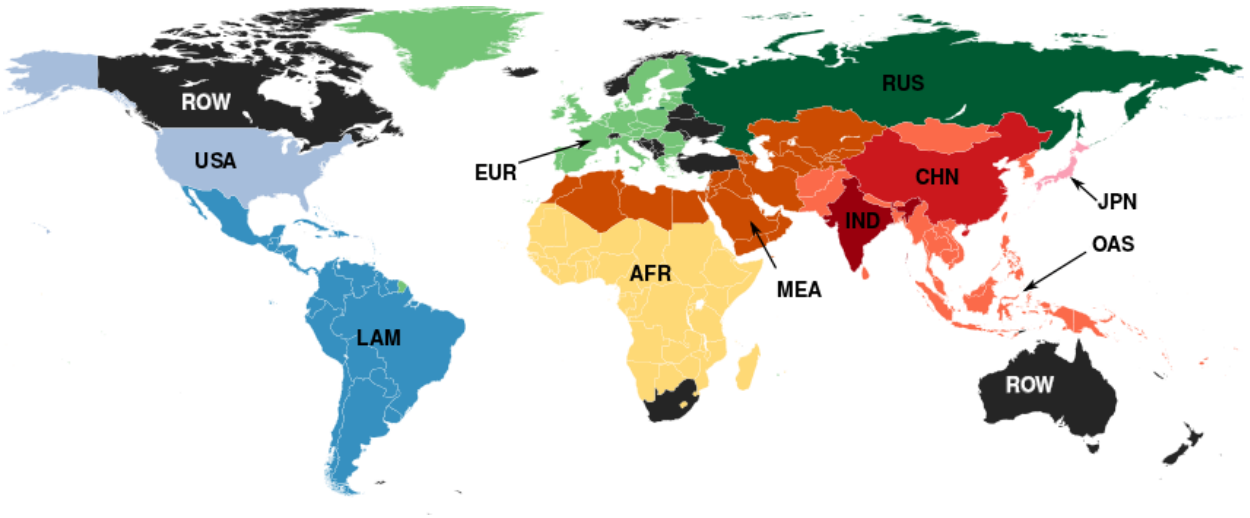


**Figure 2: Regional definitions used in the REMIND model.**

In the REMIND model, the world is broken down into 11 regions (Figure 2): five individual countries (CHN - China, IND - India, JPN - Japan, USA - United States of America, and RUS - Russia) and six aggregated regions formed by the remaining countries (EUR - Europe, LAM - Latin America, AFR - Sub-Saharan Africa excluding South Africa, MEA - Middle East / North Africa / Central Asia, OAS - other Asian countries mainly located in South East Asia, and ROW – the rest of the world including Canada, Australia, New Zealand, Norway, South Africa).

The wide scope of global energy-economy-climate models such as the REMIND model limits their level of detail. The relatively coarse regional resolution comes with methodological challenges in particular with regard to power sector modelling, which we briefly describe here and discuss in more detail in the limitations section 2.6.

Future research will likely collect, derive and employ better data, achieving a higher spatial differentiation when representing heterogeneous integration challenges and options. Our parameterization already shows substantial differences between most model regions, which is a substantial improvement over previous region-independent parameterizations. Even though some REMIND model regions are very large and consist of more than one country, they represent groups of countries that have economic, cultural and climatic similarities and are likely to improve their grid connection over time. Only for the two model regions OAS (other Asian countries) and ROW (rest of the

world) most countries do not share a border[8] and thus will not be grid-connected in the future. For these regions, we use data from a similar country as a proxy (see section 2.3).

Each REMIND region can only be represented by a single region-specific RLDC. Since substantial transmission grid expansion has been found to be a no-regret option for smoothing variability and thus reducing VRE integration challenges [24]–[27], we assume that over the next decades, transmission grids are expanded within each region, virtually making it a "copper plate". Accordingly, we spatially aggregate the time series for wind, solar and load for each region to derive RLDCs. While this "copper plate" assumption is not too far from today's state in countries of limited size (e.g., France, Spain, Germany), it requires substantial transmission grid expansion in larger regions, such as the EU, US, or China.

REMIND represents grid costs in an aggregated way, as the spatial aggregation in the model rules out an explicit representation of individual transmission grid lines. Grid investments are accounted for via two generalized grid cost mechanisms: A first flat grid cost component reflects the costs of well-developed transmission and distribution grid infrastructure seen today e.g. in the US or the EU. This cost is calculated based on the total electricity demand, without differentiating from which source it is provided, and amounts to 25-30$/MWh[9]. On top of these general cost associated with all electricity use, we add a second grid cost component that only applies to electricity produced from VRE, and which represents an additional expansion of long-distance transmission grids within each region to better integrate VRE. For this, we use an approach presented in Ref. [28], with grid costs updated based on recent REMix runs for Europe [29], leading to average VRE grid cost markups of 6-23$/MWh.

### 2.2. Scenario definition

To analyze the deployment of VRE in REMIND, we use three scenarios: a scenario with no long-term climate mitigation policies ("Baseline") and two scenarios with stringent climate policies, one with a wide range of technology options ("Tax30 scenario") and one with limited CCS and nuclear deployment ("RE Tax30"). More specifically, the RE Tax30 scenario prohibits new CCS and nuclear power plants after 2020 and analyzes the resulting effect on VRE deployment.

For the two policy scenarios the model assumes a carbon tax of 30 $/tCO$_2$ in 2020, increasing at 5% per year, implying a >66% chance of achieving the 2°C target. The relevance of the Tax30 scenarios does not rely on the global implementation of a high carbon tax until 2020. Instead, the carbon tax has the methodological purpose of deriving an optimal climate mitigation scenario in line with the 2°C target. Also, the carbon tax mimics a form of stringent global climate policy. While economic theory suggests that carbon pricing is the most efficient way of reaching ambitious climate targets, Bertram et al. [30] show that a mix of low-carbon support, regulation of fossil investments in combination with a low carbon price , can initiate a similar transformation of the global energy system at limited efficiency losses.

[8] Note that this is the case for any global modeling attempt.
[9] All $ values are in US-$ for 2015.

### 2.3. Input data: Global load and VRE supply time series

A region-specific model representation of integration challenges in a global model like REMIND requires regional data for a range of world regions. We implement region-specific RLDCs into the REMIND model to represent the temporal matching of load and VRE supply. For deriving these RLDCs (including the impact of storage), the DIMES model needs an input of three time series per region: load, wind power and solar PV power, each with hourly resolution. While VRE supply data is increasingly available for more and more world regions, load data is scarce, in particular for developing and emerging economies such as African countries, India, Brazil or China.

The RLDC data (derived from hourly wind, solar and load data for the different world regions) as well as the region-specific time series for wind and solar are available in the supplementary material of this paper. In addition, we indicate the sources of the underlying original load time series.

The load data are historical time series, mostly for one or more years, in hourly resolution. For the development of the RLDCs, we used these load profiles, thus implicitly assuming that they will retain their current shape for the full time horizon of the model. Estimating and incorporating future changes of temporal load profiles is a complex issue and beyond the scope of this paper. We discuss the potential impact of this simplification and directions for future refinements in the limitations section 2.6.

Table 1 gives an overview on the load data and Table 2 on the VRE supply data. We derived region-specific RLDC parametrizations for eight REMIND model regions (column 1) based on collected VRE supply and load time series with hourly resolution. Some regions' load data time series needed to be approximated from data that only covers a part of the respective model region due to lacking load data. Latin America was parameterized on the basis of Brazilian load data only; Sub-Saharan Africa by aggregating country load data for Ivory Coast, Ghana, South Africa; load data for China by a reference load day; and the Middle East / North African / Central Asia model region by an aggregation of Algeria, Egypt, Israel, Jordan, Lebanon, Morocco, Syria and Tunisia. Three REMIND model regions have no individual parameterization due to lacking load data. They are approximated by the representations of related model regions (Europe is used as a proxy for Russia, India for Other Asia, USA for Rest Of the World ROW).

**Table 1: Overview on the hourly time series data for load data, which was collected to parameterize RLDCs for different REMIND model regions.**

| | RLDC region | used for REMIND model region | Parameterization based on data aggregated from these countries | Data source | Year | Comment |
|---|---|---|---|---|---|---|
| Load data | USA | USA, ROW | USA | EPRI (personal correspondence)<br><br>aggregated from FERC data: http://www.ferc.gov/docs-filing/forms/form-714/data/form714-database.zip | 2010 | |
| | EU | EUR, RUS | European countries | German Aerospace Center (DLR) (personal correspondence)<br><br>aggregated from ENTSO-E: https://www.entsoe.eu/data/data-portal/consumption/Pages/default.aspx | 2006 | |
| | Middle East & North Africa | MEA | Algeria, Egypt, Israel, Jordan, Lebanon, Morocco, Syria, Tunisia | German Aerospace Center (DLR) (personal correspondence)<br><br>based on Ref. [31] | 2004-2006 | For most countries, the full load curve was interpolated from a number of reference days |
| | China | China | China | Energy & Resources Group - University of California, Berkeley (personal correspondence)<br><br>Based on Ref. [32]–[34] | 2008 | Consists of a reference day scaled to different heights for each month |

| | | | | | | |
|---|---|---|---|---|---|---|
| Load data | Latin America | Latin America | Brazil | Operador Nacional do Sistema Elétrico (ONS)<br>(personal correspondence) | 2009 | |
| | Sub-Saharan Africa | Sub-Saharan Africa | Ivory Coast, Ghana, South Africa, Middle East/North Africa | IRENA<br>(personal correspondence) | 2008 (Ivory coast)<br><br>2009 (Ghana)<br><br>2010 (South Africa) | To represent the load pattern of northern and eastern African countries, MENA time series contribute 1/4th to the aggregation |
| | Japan | Japan | Japan | METI<br>(personal correspondence) | 2010/2011 | Anomalous data for March 2011 due to Great East Japan Earthquake was replaced by data from February 2011 |
| | India | India, Other Asia | India | Central Electricity Authority (CEA)<br>(personal correspondence)<br><br>http://www.cea.nic.in/archives.html | 2010 | |

**Table 2 : Overview of the hourly time series data for VRE supply data, which was collected to parameterize RLDCs for different regions REMIND model.**

| | RLDC region | used for REMIND model region | Parameterization based on data aggregated from these countries | Data source | Year |
|---|---|---|---|---|---|
| VRE supply data (wind on- and offshore, solar PV and CSP) | USA | USA, ROW | USA | German Aerospace Center (DLR) (personal correspondence)<br><br>Based on Ref. [35] | Data of one representative year based on irradiation and wind speed data for 1984 - 2005 |
| | EU | EUR, RUS | European countries | | |
| | Middle East & North Africa | MEA | Algeria, Bahrain, Egypt, Iran, Iraq, Israel, Jordan, Kuwait, Lebanon, Libya, Morocco, Occupied Palestinian Territory, Oman, Qatar, Saudi Arabia, Sudan, Syrian Arab Republic, Tunisia, United Arab Emirates, Western Sahara, Yemen | | |
| | China | China | China | | |
| | Latin America | Latin America | All South American and Middle American countries | | |
| | Sub-Saharan Africa | Sub-Saharan Africa | All African countries not in Middle East & North Africa | | |
| | Japan | Japan | Japan | | |
| | India | India, Other Asia | India | | |

Global time series of hourly power generation with VRE technologies (open-area PV, CSP, onshore and offshore wind) are generated with the REMix Energy Data Analysis Tool. The data base comprises a time period from 1984 through 2005. For a detailed description of input data, methods and the tool itself see [35]. The hourly power generation potentials are analyzed in three steps: land use assessment, resource data analysis and application of a power plant model.

The global land use assessment comprises the analysis of suitable areas at 300x300m resolution, employing the Global Land Cover database [36]. The following types of land use are considered: herbaceous or sparse vegetation, bare areas, and shrub land. These areas are reduced by glaciers, sand

dunes, saltpans, water-covered areas, protected areas, settlements and areas with a slope exceeding a technology-specific maximum.

The resource data analysis uses data from [37], which are used to derive hourly global horizontal and beam normal irradiance values which are required as input into the PV and CSP power plant models. Wind speed data 50m above ground retrieved from [38] are converted to wind speed values at hub height and used as input for the wind turbine model. The power plant models define area-specific installable capacities, efficiencies of the energy conversion and, in case of CSP, efficiency of storage, availability, life times, as well as investment and operation costs. Maximum installable capacities in each suitable raster cell are calculated by multiplying its area with the area-specific installable capacity. This capacity value and the resource information are then used to calculate hourly maximum power output in a raster cell.

### 2.4. Parameterizing the impact of short-term storage with the DIMES model

Short-term storage is an important option for facilitating the integration of VRE, or equivalently increasing the economic value of VRE. However, explicitly accounting for storage and its detailed operation within the REMIND model would be highly challenging if possible at all, as it would require close to hourly temporal resolutions[10]. We estimate the role of storage with the separate DIMES model and derive an extensive set of RLDCs containing the impact of storage to parameterize the REMIND model. REMIND then accounts for the costs of storage capacity and the benefits from storage in terms of a less challenging RLDC. DIMES runs were conducted for gross wind and solar shares, each between 0 and 120%[11], and for eight out of eleven REMIND model regions[12] resulting in 1352 model runs.

The RLDC data derived for the different world regions is available in the supplementary material of this paper, thereby allowing other modelling teams to adopt this approach for their models, or to inform alternative approaches for representing variability.

The **D**ispatch and **I**nvestment **M**odel for **E**lectricity **S**torage (DIMES) is numerically lean, allowing for a large number of model runs, e.g., for sampling a large parameter space, while representing the relevant details for parameterization of the REMIND model. It is a stylized numerical dispatch and investment model of the power sector that is not calibrated to a specific region, but can be fed with hourly VRE supply and load data from different regions. In a linear optimization it minimizes total costs of power supply (investment, operation & maintenance, and fuel costs) by determining investment (i.e. a green-field approach) and dispatch of non-VRE power capacity as well as short-term storage capacity and

[10] In addition to price differentials (« spreads ») between times of high residual load and low residual load or overproduction, the economics of short-term storage is determined by the number of charge-discharge cycles it operates over the year.

[11] Throughout the paper *share* of VRE is defined as generation share of total annual load. In the « gross share » values, overproduced VRE generation from VRE supply exceeding load (negative part of RLDC) is also counted, so these values can become larger than 1. « Net share » values count only the VRE generation that can be used, and thus cannot be larger than 1.

[12] As described in section 2.3, three REMIND model regions have no specific parameterization due to a lack of load data. They are approximated by the representations of related model regions (Europe is used as a proxy for Russia, India for Other Asia, USA for Rest Of the World).

reservoir size based on an evaluation of one year in hourly resolution. Investments are calculated based on annualized costs. All generation and storage technologies are represented by their specific techno-economic parameters (e.g. efficiency, fixed and variable cost, emissions, life time) and their aggregated capacity, i.e., single plants and units are not resolved. The model does not resolve grid lines, but uses a copper plate assumption in accordance to the REMIND model (see last paragraph in section 2.1). The generic short-term storage in DIMES was parameterized based on the techno-economic properties of flow batteries expected for 2050 as seen in REMIND, [28]. Assumed capacity costs are 310$/kW, reservoir costs are 100$/kWh and round-trip efficiency is 76%. All DIMES runs assume a carbon price of 150$/t$CO_2$, which is in line with 2050 carbon prices in scenarios consistent with the 2°C target.

Figure 3 illustrates a typical RLDC result derived for Europe by sorting the hourly dispatch results of DIMES. The LDC (load duration curve) changes to an RLDC with increasing VRE share (here shown: 80% PV and 20% wind power). Two RLDCs are shown: One without and one with short-term storage. The DIMES model endogenously decided on the cost-optimal amount of storage capacity to reduce integration challenges. Storage allows the use of parts of VRE generation that would be over-produced without storage. As a result, both curtailment and residual peak load decrease.

To validate the one-node approach (no grid representation) of DIMES, we compare the DIMES RLDC results to the output of the REMix model. REMix is a highly sophisticated dispatch and investment model that applies more detail, such as a differentiation of 15 regions with specific load and VRE supply data ([29], [39]). While REMix is useful as a validation for DIMES, it could not be used to parameterize all world regions, as REMix's geographical coverage is limited to Europe.

While the results were already quite similar in the basic version, we could improve the matching between DIMES and REMix by splitting the short-term storage in DIMES into two separate technologies with costs varied by ±20%, and allowing the model to use the storage technology with lower costs only for supplying the first 50% of peak load. This split is a simple representation of the fact that in a one-node model, storage can be used to equilibrate any over/undersupply, while in a 15-node model with explicit grid costs, the marginal value of storage decreases with increasing storage deployment: the more storage is deployed, the more it could be used to equilibrate over/undersupply in different regions, which leads to increased transmission costs and losses.

Figure 3 visualizes the general effect of storage on the RLDCs by comparing outputs derived from the DIMES model to those of the more detailed REMix model. We find that DIMES RLDCs including storage are in decent agreement with those derived from REMix. Due to the country heterogeneity in REMix, the REMix RLDCs are much smoother and do not show the steps visible in the DIMES RLDCs; however, residual peak load, curtailment, and the general shape of the RLDCs are in good agreement.

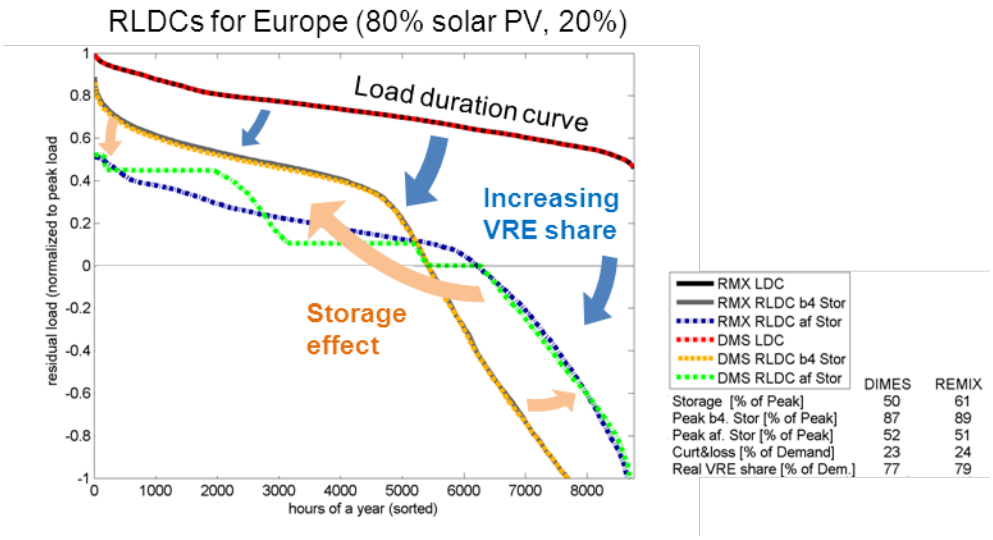


Figure 3: LDC and RLDCs with and without storage operation for DIMES and REMix for Europe.

## 2.5. Implementing RLDCs in REMIND

The core of the RLDC approach is a representation of RLDCs in the REMIND model. Different approximations of the RLDC shape and ways of implementation are suggested in [15]. We use a numerically lean step-wise approximation based on four rectangular "load bands", which we term "peak-load band", "higher mid-load band", "lower mid-load band" and "base-load band"; as well as two additional variables for residual peak load (maximum residual load over one year) and curtailment. This allows for a fairly good approximation of RLDCs while the additional numerical complexity is still manageable.

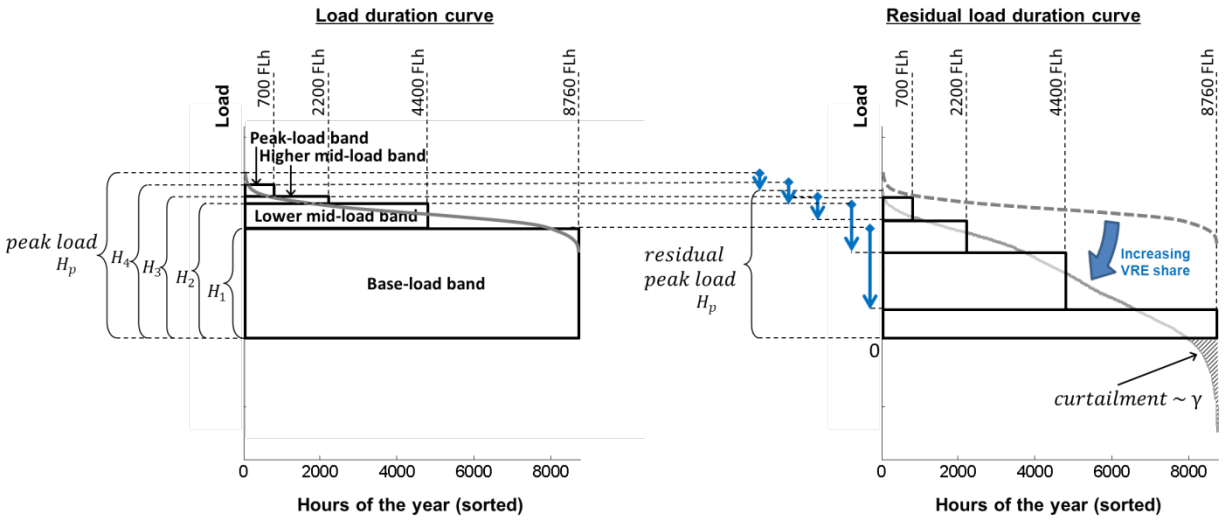


Figure 4: Sketch of the model approximation of RLDC at 0% VRE, i.e. load duration curve, (left) and an RLDC at about 40% VRE (right). Four rectangular "load bands" and the residual peak load endogenously change in response to wind and solar deployment. In addition, the negative part of the RLDC indicates VRE supply that exceeds demand. It is termed "curtailment" here and can be used as an input to storage.

Figure 4 illustrates the RLDC approximation. The four load bands are characterized by their full-load hours (FLH) and capacity factor (determining the load band widths), which are fixed. By contrast, load band heights change depending on the gross share and mix of VRE. Without VRE generation, the heights of the load bands are fitted to the region-specific LDC (Figure 4, left). With increasing VRE share, the height of each load band changes (blue arrows in Figure 4, right). Also the residual peak load $H_P$, which determines the required non-VRE capacity (see the capacity equation (6) in Appendix A.2), decreases with increasing VRE share.

The changing shape of the RLDCs is parameterized in REMIND in two steps:

1) Every RLDC (output from the DIMES model) is fitted by the four load bands such that the deviation between the load band step function and the actual RLDC data is minimized. For each region, gross wind and solar shares are varied from 0% to 120% in 10% steps, which results in $13^2 = 169$ combinations. The fitting procedure results in six parameters characterizing the RLDC shape: the height of each of the four rectangular load bands $H_{1..4}$, the residual peak load $H_P$ and curtailment rate $\gamma$ (curtailed share of gross VRE generation).
2) To implement the changing RLDC shape, two-dimensional functions depending on gross wind and PV share are derived for each of the six parameters and each region. Each function is a polynomial of the two variables wind and solar share with polynomial coefficients derived from fitting the 169 data points that span the range of wind and solar power (see for example Figure 5).

All polynomial coefficients are given in Table 5 in the Appendix A.1 and the core equations of the implementation are explained in A.2.

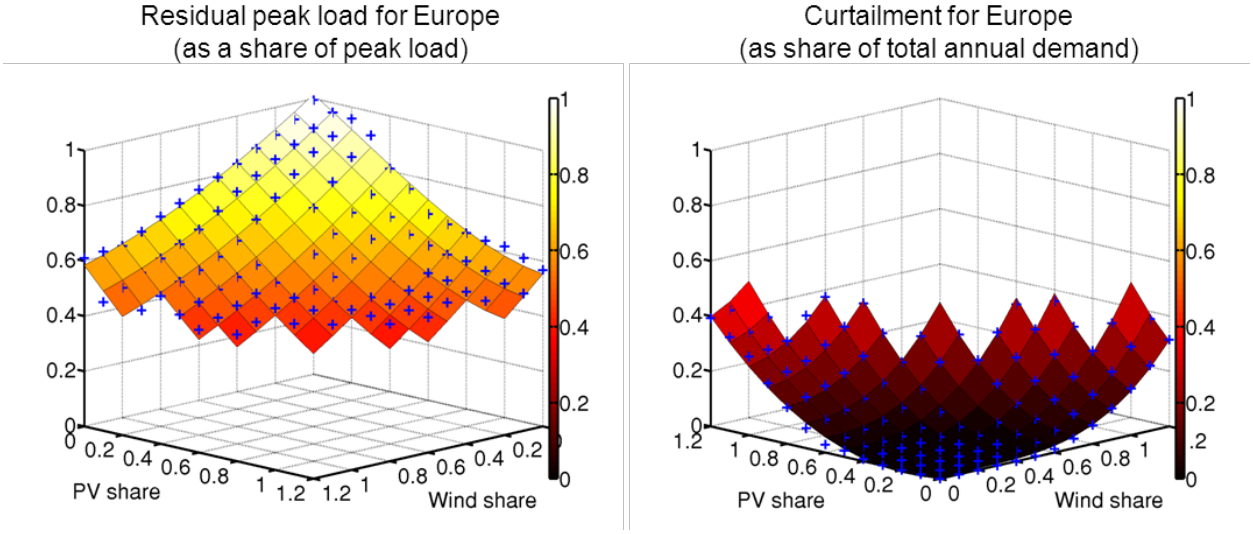


**Figure 5: 2-dimensional fit of residual peak load as share of peak demand (left) and curtailment as share of total annual demand (right) dependent on the gross share of PV and wind for the EU. The results from individual DIMES runs are represented by blue crosses, the colored surface represents the polynomial fit. To improve visibility, the share of PV increases towards the viewer in the left figure, while it increases away from the viewer in the right figure. The thin black lines on the coloured surface represent the 10%-steps in PV and wind share, so that at each crossing of two black lines, one DIMES run yields an RLDC, from wich a value for the analyzed variable is extracted. In case of a perfect fit of the 2D-function**

**to the DIMES results, each blue cross would be partially visible and situated at the crossing of two black lines. If the blue cross is fully visible, the DIMES value is higher than the 2D-fit, and vice versa.**

As an example, Figure 5 shows the parameterizing functions for the residual peak load (left) and curtailment (right) parameters for a range of gross wind and solar shares for Europe. The comparison of the third-order polynomial fit (colored surface) to the original data (blue crosses) shows good agreement. The blue crosses should ideally match the crosses of the lines. Increasing the polynomial degree of the fitting function would increase both fit accuracy and model complexity. Considering this tradeoff we chose a third-order polynomial with mixed terms. All fits used for REMIND have a coefficient of determination $R^2$ better than 0.83, with all load band fits having an $R^2$ of 0.96 or better.

As a result of the new implementation, the RLDC approach allows the REMIND model to more accurately determine the cost-optimal deployment of both VRE plants and non-VRE plants under consideration of their most important interactions. Wind and solar plants are endogenously deployed with full anticipation of the challenging VRE impacts captured in RLDCs, i.e., a rather small VRE capacity credit, the reduced utilization of dispatchable plants and over-produced VRE generation, which might need to be curtailed. It therefore also accounts for the diminishing marginal value of VRE generators due to self-correlation within VRE generation [11], [13]. Analogously, when investing in dispatchable power plants, the model considers the long-term capacity requirements for covering residual load - from base load to peak load. This includes the long-term reduction of annual FLH (i.e. capacity factors) over the lifetime of dispatchable plants due to increasing VRE share, which typically induces a shift from base load plants to peak load plants.

Short and long-term storage technologies are modelled differently in the RLDC implementation presented here. The impact of short-term storage is already accounted for in the parameterization of the RLDCs based on DIMES, because its representation requires a much higher temporal resolution of close to hourly detail in combination with full information on temporal ordering, which is both not contained in the RLDCs anymore. By contrast, long-term storage is endogenously represented in the REMIND model as described in Ref. [15]. Overproduced VRE generation can be transformed into hydrogen via electrolysis. Hydrogen can be directly used, e.g., in the transport sector, or used to generate power in times of higher demand via hydrogen turbines or co-firing of CSP plants. The key determinant for the economic efficiency (and profitability) of installing electrolysis capacity is the amount of available overproduction and the resulting capacity factor of the electrolysis. Both depend on VRE share and mix and are captured in the negative part of the RLDC. The RLDC representation allows REMIND to endogenously choose the optimal amount of long-term storage.

### 2.6. Limitations and future refinements

Like any reduced-form representation, the RLDC approach has shortcomings, which we discuss in the following paragraphs. Note that some of these shortcomings apply to long-term models in general and point to promising fields of further methodological research.

By using duration curves, information about the temporal sequence for generation and demand is lost. This hinders a direct and accurate representation of some aspects that depend on short-term dynamics

such as the flexibility[13] of non-VRE generation. In general, any long-term energy model without explicit representations of sub-hourly time-scales cannot guarantee that there is sufficient flexibility to reliably balance supply and demand. Other highly-resolved production cost models are designed for this purpose, which can validate the results of a long-term model. This has been done for long-term energy models that represent single countries (see for example Ref. [40]–[42]). Doing so for a global model with multiple regions requires significant processing effort (requiring a model calibrated for each region), which is why, to our knowledge, such a global validation has never been done. However, we believe that also without bottom-up validation the resulting error is small for global models that use the presented RLDC approach for three reasons:

1) Accounting for RLDCs alone already incentivizes investments in more flexible thermal plants. The reduced utilization of thermal power plants induces a shift towards less capital-intensive intermediate and peak load power plants, which are generally more flexible than base-load plants.
2) The presented approach requires the installation of short-term storage in the form of flow batteries at higher VRE shares. Such batteries are very flexible and could partially compensate for limited flexibility in the residual system.
3) Many studies show that the costs for providing additional flexibility with increasing VRE shares are low, i.e., less than 6 EUR per MWh of VRE (<10% of VRE generation costs) at VRE shares of up to 40% ([12], [13], [43]), compared to other integration cost components. The substantial uncertainties of future technology costs are much larger than these additional costs, which will therefore only have a minor effect on the findings derived from long-term scenarios.

Another short-term aspect in time scales of seconds and even milliseconds is not represented in the RLDC approach. VRE generators are connected to the grid in a non-synchronous way, in contrast to conventional generators, where the mechanical rotation of the turbine is coupled to the system's electrical frequency. This decreases power system's inertia and thus could endanger power system's stability in case of high instantaneous VRE penetrations. A study for the 2020 Irish power system estimated a restriction on the instantaneous system non-synchronous penetration (SNSP, the sum of non-synchronous generation sources like wind or PV) of 70% in case no alternative inertia is added to the system such as emulated inertia from wind turbines [44]. Since 2011, Eirgrid is working on increasing the SNSP limit from the current value of 50% to 75% in 2020 [45]. As advanced VRE generators and other technologies such as fly-wheels or batteries increasingly contribute to frequency control [46], we expect that the limit to instantaneous VRE penetration will be pushed even higher in future power systems. Hence, we expect that neglecting this issue does not affect the validity of the RLDC approach.

To our knowledge, this paper is the first to collect and implement VRE supply and load data at high temporal resolution for most world regions. While this is a substantial advance from previous model analyses, future refinements need to be made to improve this parameterization:

[13] Flexibility refers to the ability of thermal power plants to adjust their generation on short notice over a wide range. Aspects of flexibility are ramping and cycling constraints, minimum electric load, minimum heat load (in case of CHP), minimum up and down times, part-load efficiency, operating reserve requirements, and corresponding costs.

1) Most importantly, better and more extensive load and VRE data is required for many world regions. Using synchronous load and VRE data from several years would improve the robustness of the RLDC parameterization, even though the deviations between RLDCs from different years with the same wind and solar share are small. In addition, due to the limited amount of load data time series currently available, we had to use load time series for individual sub-regions or countries as proxy for a whole region, or, in the case of China, only one representative load day.

2) The RLDC parameterization used in this paper is based on current demand profiles, while the scenarios cover the whole century. The approach could be improved by accounting for future changes in demand profiles, e.g. due to economic development and structural changes in electricity demand. This is not an inherent limitation of the RLDC approach, but rather points to a more fundamental challenge of deriving appropriate projections for input parameters in long-term scenario analyses. We discuss the potential impact of the simplification and directions for future refinements.

   There are several drivers that change demand profiles and thus affect their matching with VRE supply. The increasing deployment of cooling systems such as air conditioning, in particular in hot developing and emerging countries, would increase the matching of load and solar, which would increase the role of solar PV. However, at high VRE shares the self-correlation of VRE generators, i.e. the matching of VRE with *residual* load, becomes more important than the matching of VRE supply with load.

   Electrification of the heat and power system is a pillar of many climate mitigation scenarios. The resulting changes to demand profiles highly depend on behavioral aspects such as battery charging patterns of electric vehicles. Regulatory, market design and technical aspects influence the flexibility[14] of the additional demand (demand response). Highly optimistic assumptions on the flexibility of demand can significantly ease matching demand with VRE supply and ease VRE integration [47], while assuming simple, uncontrolled demand profiles of e.g. heat pumps and electric cars tends to increase demand in peak load times when power capacity is already scarce (as estimated for UK, Germany, and Denmark in [48]–[50]) which in turn complicates VRE integration.

   While most literature points to the need for and high potential of demand response, this remains a complex and uncertain issue. We suggest that our approach of using historic demand profiles for the future is a rather conservative assumption as it underestimates the potential for demand response especially in the far future. Conducting sensitivity studies on future demand profiles and their flexibility is a promising direction for methodological refinement of the RLDC approach and for further research in general. Ideally, modelled load profiles should change endogenously depending on the sources of electricity demand; yet this level of detail is hard to achieve in global energy-economy-climate models. As an alternative, demand response can be parameterized exogenously by a highly-resolved model for a range of VRE shares and mixes, similar to the one used for short-term storage in this study.

[14] Flexibility here refers to both the share of demand that can be shifted in time and the duration of these shifts.

Another important methodological challenge that all global energy-economy-climate models have in common is their high spatial aggregation e.g. the REMIND model divides the world into 11 large regions. In the following we discuss resulting limitations with respect to i) finding a representative RLDC for each region and ii) considering grid investments in the model.

1) We spatially aggregate the time series for wind, solar and load for each model region to derive region-specific RLDCs and hereby assume perfect transmission within each region. Such a copper-plate assumption is an optimistic assumption for most regions in the near future, and also in the long-term future for large regions with weak current infrastructure such as Sub-Saharan Africa. On the other hand, we argue that some additional aspects of our implementation, the scenario design and the role of grid expansion prevent an overly optimistic bias in our scenario results and on balance create a reasonable set of assumptions.

   Becker et al. [25] analyze the effect of transmission grid expansion for increased wind and solar integration in the EU. They find that even a four-fold increase of todays net transfer capacities is sufficient to reap 90% of the maximum integration benefits that would be achievable through a copper-plate EU. This result suggests that the copper-plate assumption used in models for simplicity reasons does not need to be understood as a perfect grid-interconnection in reality, but as a proxy for ambitious transmission grid expansion.

   Such transmission grid expansion has been found to be a no-regret option for smoothing variability and thus reducing VRE integration challenges [24]–[27], making it a likely part of cost-optimal climate mitigation scenarios. The costs for such a transmission expansion are much smaller than the costs for transforming the generation part of the energy system in a low-carbon scenario ([27], [41]). This is also true in terms of long-term total system costs[15] and thus transmission expansion seems to be a no-regret option for regions beyond those that already have a well-developed transmission infrastructure.

   Different world regions clearly differ in the rate at which transmission grid infrastructure can be expected to be built up and then match our pooling assumption for load and VRE supply. For the US and EU it seems likely that transmission grids will be significantly expanded within the next 2-3 decades in accordance with increasing VRE generation. NREL finds that new transmission is substantial for an 80%-renewable scenario of the US power sector, but estimated transmission investments are in line with recent historical trends [41]. For regions with a weak current infrastructure and higher institutional barriers to grid extension, an extensive interconnection will take longer, probably until 2050, and thus assuming such an interconnection already in the first half of the century is optimistic and neglects some sub-regional diversity in integration challenges. However, we suggest that the resulting bias of scenario results is rather small because i) integration challenges are small at rather moderate VRE shares until 2050 and ii) the REMIND model aims at analyzing cost-optimal energy system transitions until the end of the century. In addition, institutional barriers that slow down grid expansion tend to be neglected in the global models that focus on a cost-efficient transition towards a low-carbon energy supply.

[15] Long-term total system costs correspond to a green-field approach without existing generation or transmission capacities.

The optimistic assumptions on pooling are to some extent compensated by the above-mentioned conservative assumptions on load flexibility. In addition, we do not always aggregate load data from the entire world region (only for EU, USA, India) and instead use a subset of countries and subregions due to a lack of data. As a result load variability is not smoothed as much as if load data from all sub-regions were available and pooled.

Ideally, RLDCs would be parameterized with detailed models for each world region that take into account the gradual expansion of transmission grids. This would add another dimension (state of grid infrastructure) to the extensive set of RLDCs and would thus increase the numerical requirements. Future refinements would need to find a stylized parameterization of the effect of grid infrastructure on RLDCs.

2) In section 2.1 we describe how VRE-related grid costs are represented in REMIND in an aggregated way through generalized transmission cost markups on VRE electricity. We use an approach presented in Ref. [28], with grid costs updated based on recent REMix runs for Europe [29] (6-11$/MWh VRE). While these detailed calculations for cost-optimal grid deployment should ideally be performed for each region, thus far there are no electricity sector models available with sufficient detail and input data for all the different world regions. While Europe with its strong North-South-duality provides a cost estimate for significant transmission grid requirements, we assumed double the European specific grid costs, to 13-23 $/MWh VRE, as a conservative estimate for larger world regions like Sub-Saharan Africa, China, or Latin America.

   In addition, we test the impact of these grid cost assumptions on the deployment of VRE by conducting a sensitivity analysis where we increase/decrease all region-specific VRE-related grid costs by a common factor. Doubling the grid costs reduces the contribution of VRE to total electricity production (2010-2100) by 13%, while halving grid costs increases it by 8% (Figure 16 in appendix A.3).

   Beyond the pure economic costs, which are represented in the model, grid expansion could also meet non-monetary barriers such as local resistance and lack of institutions, which are very challenging to represent in highly aggregated energy-economy-climate models.

   In addition, the REMIND model does not represent electricity trade between the 11 world regions. The main reason is that the chronological order of load and VRE supply is lost in the RLDCs, and consequently the RLDCs of connected regions are not synchronous in time, which would be required for representing power transmission. The RLDC approach is most suitable to represent a single region or regions that do not transfer significant amounts of electricity between them. This is the case for most global long-term models, which typically represent the world in aggregated macro-regions that hardly trade electricity.

# 3. Results

This section has two parts. In section 3.1 we discuss how integration challenges, i.e. the matching of VRE supply with load, differ (and do not differ) between regions, VRE mixes and shares. We show regional RLDCs that were used to parameterize REMIND and discuss the impact of short-term storage. In section 3.2 we show REMIND scenario results based on the implemented RLDC approach and relate the results

to the region-specific integration challenges discussed in 3.1. For all results, we focus on Europe, USA and (Sub-Saharan) Africa because they show a range of integration challenges as they are characterized by different seasonal and diurnal matching properties of wind and solar power with load.

### 3.1. Regional VRE integration challenges captured in RLDCs

This section shows a range of RLDCs for different regions and VRE technologies, with and without diurnal storage. The RDLCs are used to parameterize the REMIND model. Hence, region-specific integration challenges and their mitigation via storage are considered in the REMIND scenario results shown in section 3.2.

Figure 6 illustrates the underlying time series data that show matching patterns of load and VRE supply that to a large extent shape RLDCs. The time series of load, wind and solar illustrate both seasonal matching (left) – based on weekly average values for one year – and diurnal matching (right) – based on average days in hourly resolution. The average days are derived for the season in which load shows its annual peak for each focus region, e.g. the summer season in the US because load is higher during the summer there. The solid line represents an average day and the $15^{th}$ and $85^{th}$ percentiles are shown with dotted lines. The three focus regions Europe, USA and Africa, show a range of distinct characteristic seasonal and diurnal matching properties, which shape the RLDCs and influence the role of short-term storage.

For the US, the annual demand peak in summer coincides with the annual solar peak, and during this peak season, the diurnal demand curve coincides with the diurnal solar curve. For the EU, annual demand peak occurs in winter, where wind also peaks. However, wind does not have a strong diurnal peak in the EU, so the diurnal matching between wind and demand is limited. In Africa, flat load coincides well with flat solar over the year, but the diurnal demand curve is also quite flat and peaks in the evening, thus being not very well correlated with solar.

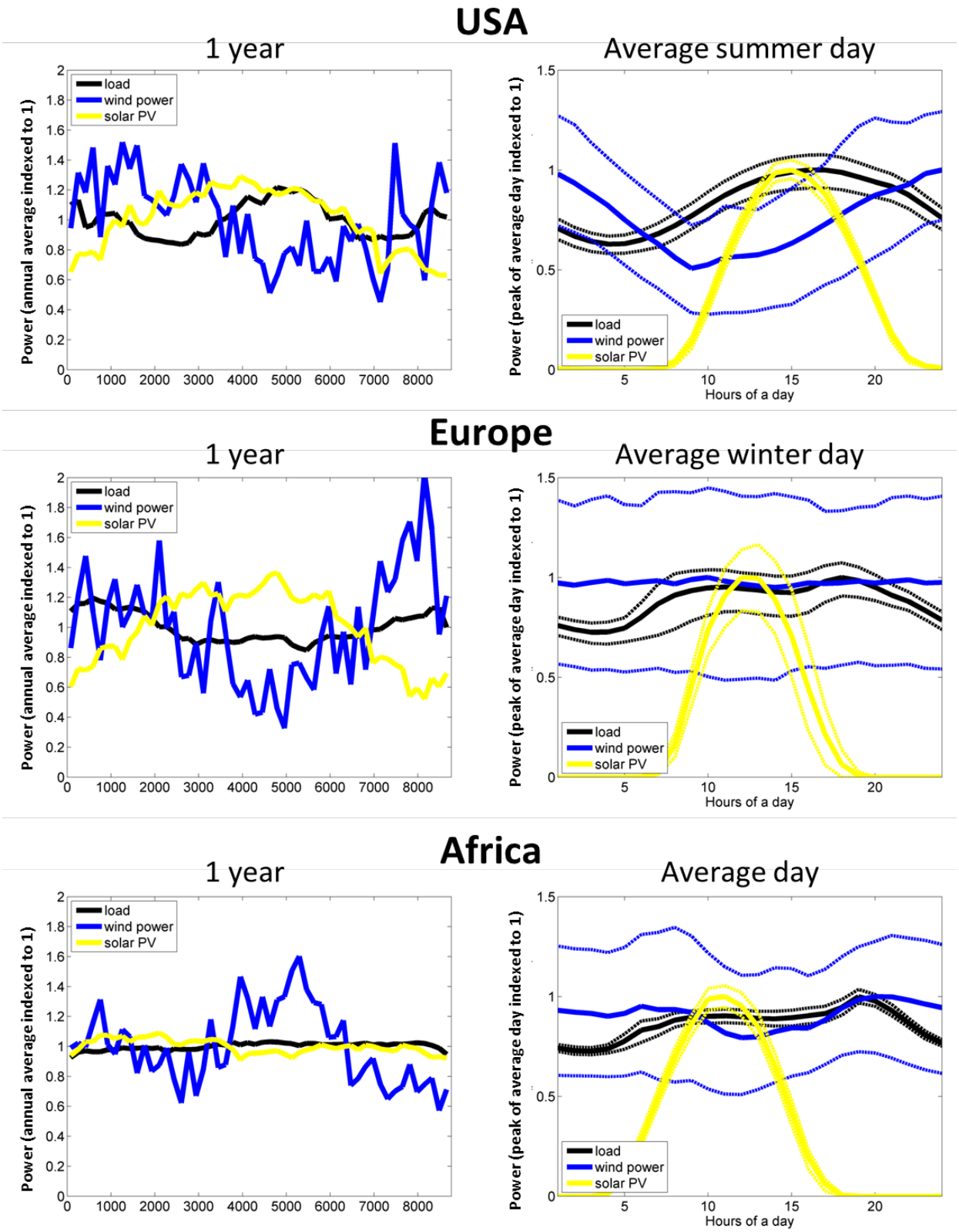


**Figure 6: Annual time series of weekly averages that illustrate the seasonal correlation of load, wind and solar (left) and diurnal time series (right) that show the diurnal matching of load, wind and solar PV for Europe, USA and Africa. The dotted lines (right) show the 15$^{th}$ and 85$^{th}$ percentiles for each average day time series.**

### *Comparing regional RLDCs for wind and solar PV*

Figure 7 shows RLDCs for all six combinations of the focus regions (Europe, USA, and Africa) and VRE technology (wind and solar PV) for increasing gross shares (0% - 100%). These curves do not yet account for the impact of storage, which is shown later in Figure 8.

The RLDCs confirm the well-established result that VRE integration challenges (as described in the introduction) increase with increasing VRE shares ([10], [12], [13], [43]). The VRE capacity credit is low or moderate at small VRE shares but vanishes with increasing shares. The FLH of non-VRE plants decrease and overproduction (negative part of the RLDC) increases at high VRE shares. As a consequence, even at very high deployment of VRE generators there is a part of electricity demand that cannot be directly met by VRE. It can only be covered by conventional thermal capacity, non-variable renewables (*e.g.* hydroelectric power) or through a temporal shift of either load (via demand-side management) or over-produced VRE (via storage).

Although the overall character of integration challenges is similar, there are some noticeable differences between wind (Figure 7 left) and solar PV (Figure 7 right). Increasing solar PV above 20%-30% creates a kink in the RLDCs around hour 4500 – a bit more than half of the year's hours. Additional solar generation beyond this threshold does not contribute to peak or intermediate load, but almost exclusively decreases the RLDC to the right of the kink such that at high shares most additional generation is over-produced. The reason is the regular day-night cycle of solar PV generation, i.e., the kink separates sun-intensive hours during daytime (right side of RLDC at high PV shares) from hours with little or no sun in the evening and at nighttime (left side of RLDC at high PV shares). Wind RLDCs do not show a kink, instead, increasing shares tend to gradually tilt RLDCs. This is because wind generation hardly follows a regular pattern (Figure 6, right). It is very stochastic in the sense that the distance between the 15$^{th}$ and 85$^{th}$ percentile of the distribution of wind power in each hour of a day is of comparable size to the mean value, and much larger than the same percentile range of solar power or load.

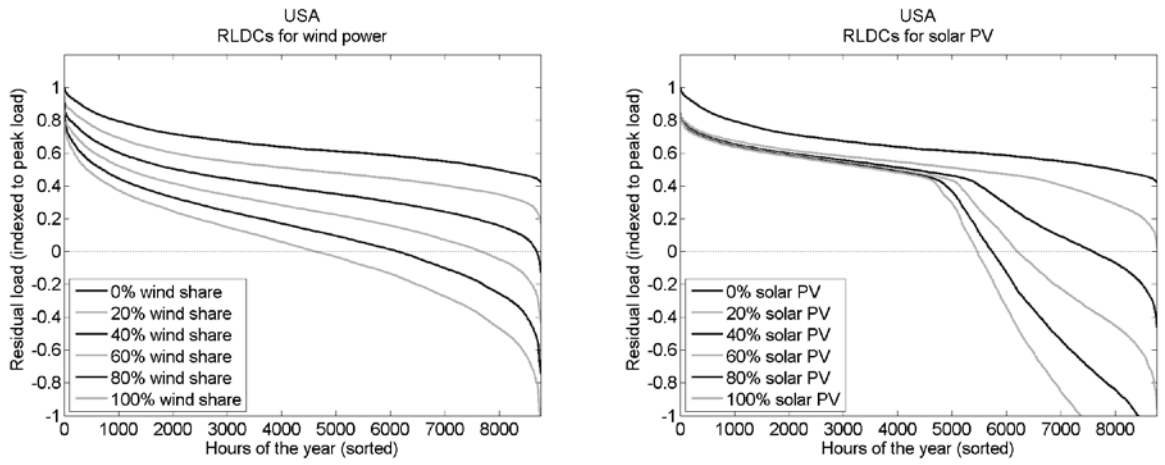

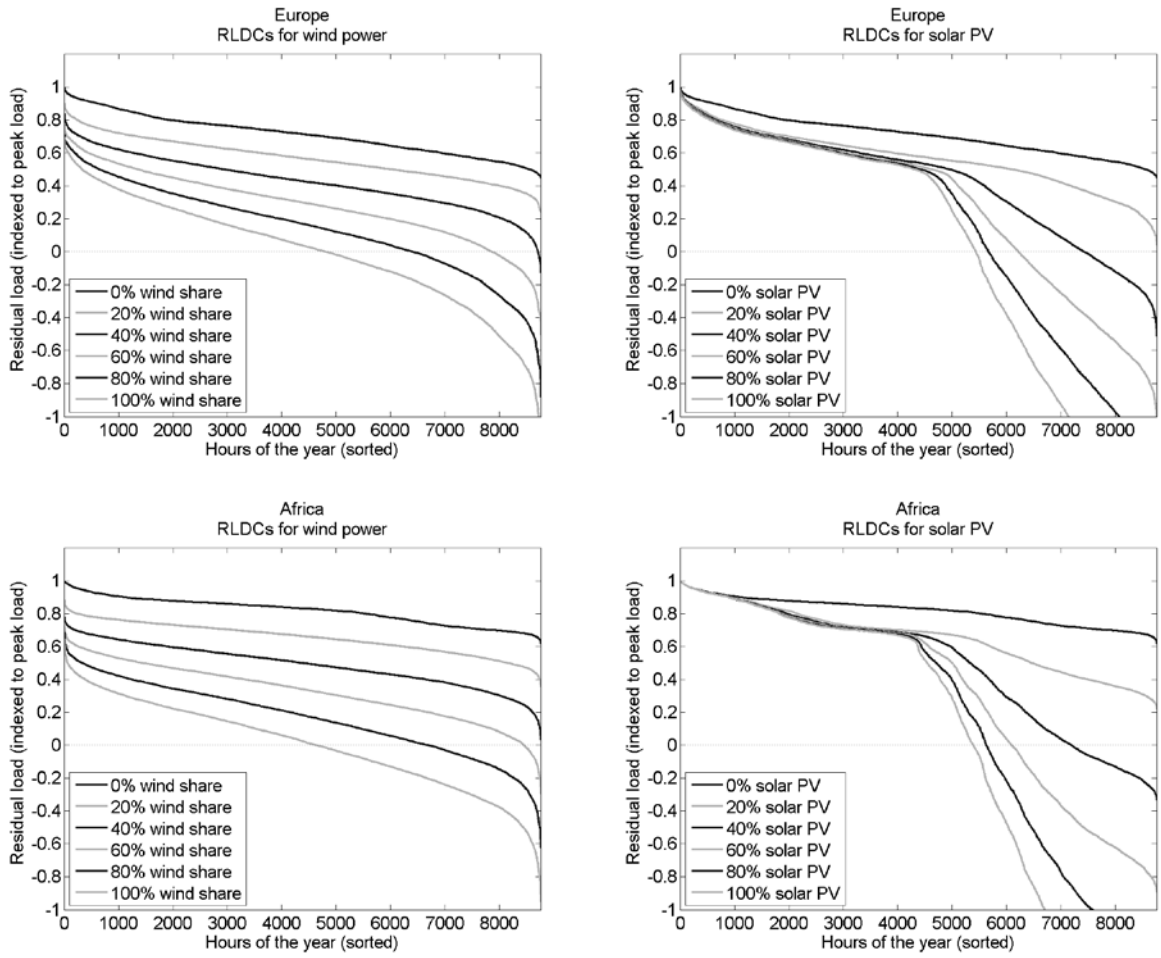


**Figure 7: RLDCs for increasing gross shares of wind (left) and solar PV generation (right) for three world regions: Europe (above), USA (middle) and Africa (below).**

While at high VRE shares (above 20%) RLDCs mainly differ between wind and solar PV, the regional differences become increasingly important at VRE shares below 20% and if storage is considered (later in this section). The reason is that with increasing VRE shares the shape of the RLDC is increasingly determined by the correlation of additional VRE generation with existing VRE generation (auto-correlation) and to a decreasing extent by the regional specific matching with load.

Without storage, RLDCs show the following regional differences for load, wind and solar PV:

- Load: Without VRE, the regional LDCs (highest curve) reflect the characteristics of the annual load time series shown in Figure 6, left: The African LDC is quite flat, while US and European load show a stronger variation between times with high and low load, indicating stronger diurnal and seasonal cycles.
- Wind: RLDCs for wind power in Africa show the highest reduction of capacity requirements and smallest curtailment with increasing wind shares, mainly because its data is based on pooling across a large and geographically diverse area. The USA RLDCs show the highest integration challenges for wind due to the diurnal anti-correlation between wind and load, while those of

the Europe are in a middle range. More specifically, from 0-20% wind share in the EU, wind power acts like a flat band that evenly reduces residual load at all times, which is based on assuming significant transmission grid interconnection.

- Solar PV: Significant regional RLDC differences occur for solar PV shares below 20%. For the US, solar PV contributes to peak load and thus reduces requirements for non-VRE capacity due to the good matching of load and solar peaks on both seasonal and diurnal scales (Figure 6). By contrast, Europe and Africa both show a low solar capacity credit, because of the bad diurnal load-supply matching in European winters, and throughout the year in Africa. Instead, solar PV contributes to intermediate load in both regions, because the mid-day peak, which is lower than the evening peak, can be met by the diurnal solar peak.

### *The impact of storage on the RLDCs*

Figure 8 shows RLDCs for increasing solar shares that include the impact of short-term storage based on the DIMES model. We only discuss results for solar PV here, because we find, based on DIMES, that short-term storage capacity hardly contributes to integrating wind power deployment if regional transmission grid expansion is assumed. This is confirmed by detailed analyses of the REMix model for Europe: long-distance transmission grid extensions are more cost-efficient than building short-term storage for integrating wind power [29]. Short-term fluctuations of wind power are smoothed out if large spatial areas are grid-connected, while the lack of regular diurnal wind patterns limits the role of short-term storage. The DIMES model further shows that there is little short-term storage in mixed wind-solar scenarios, because wind power decreases the regular diurnal pattern of load. In cases of high VRE shares with a large contribution from wind power, other types of storage with lower reservoir costs that operate on longer time scales, i.e. seasonal storage, might be more beneficial. The REMIND model contains a representation of long-term storage via electrolysis following the approach of Ref. [15].

The discrete plateaus of residual load in Figure 8 are carved out by the operation of storage, which is optimized in the DIMES model such that it minimizes total system costs. Each technology in the mix of non-VRE technologies, such as coal power plants or a gas combined-cycle plant, is most competitive to operate at a specific number of annual FLH (corresponding to a specific width of the RLDC). Storage capacity shifts electricity such that plateaus emerge, which separate load bands with a specific width (number of annual FLH) that are covered by respective non-VRE capacities. In the real world, two aspects would reduce the pronounced plateaus and result in smoother RLDCs. First, the analysis neglects some heterogeneity of power plants of the same power plant type due to different designs, build years and operation styles. Second, a detailed representation of transmission grids and the spatial distribution of storage units would account for the real-world tradeoff of transmission losses, when transmitting power to and from storage units, and the benefits of storing.

Short-term storage significantly reduces solar PV integration challenges, which can be seen when comparing Figure 8 with solar RLDCs without storage (Figure 7, right). The combination of PV with short-term storage contributes to meeting peak demand, accordingly the peak of the residual load decreases. In addition, overproduction is significantly reduced. In a first approximation, storage tends to shift electricity such that the resulting solar RLDCs become similar to those of wind. Integration challenges and resulting integration costs become roughly comparable between wind and solar-with-storage

scenarios. Hence, the cost-efficient mix of wind and solar PV is roughly determined by a simple comparison of levelized costs of electricity (including storage costs for solar PV). Without considering short-term storage, models-based analyses might underestimate the economic potential of solar PV.

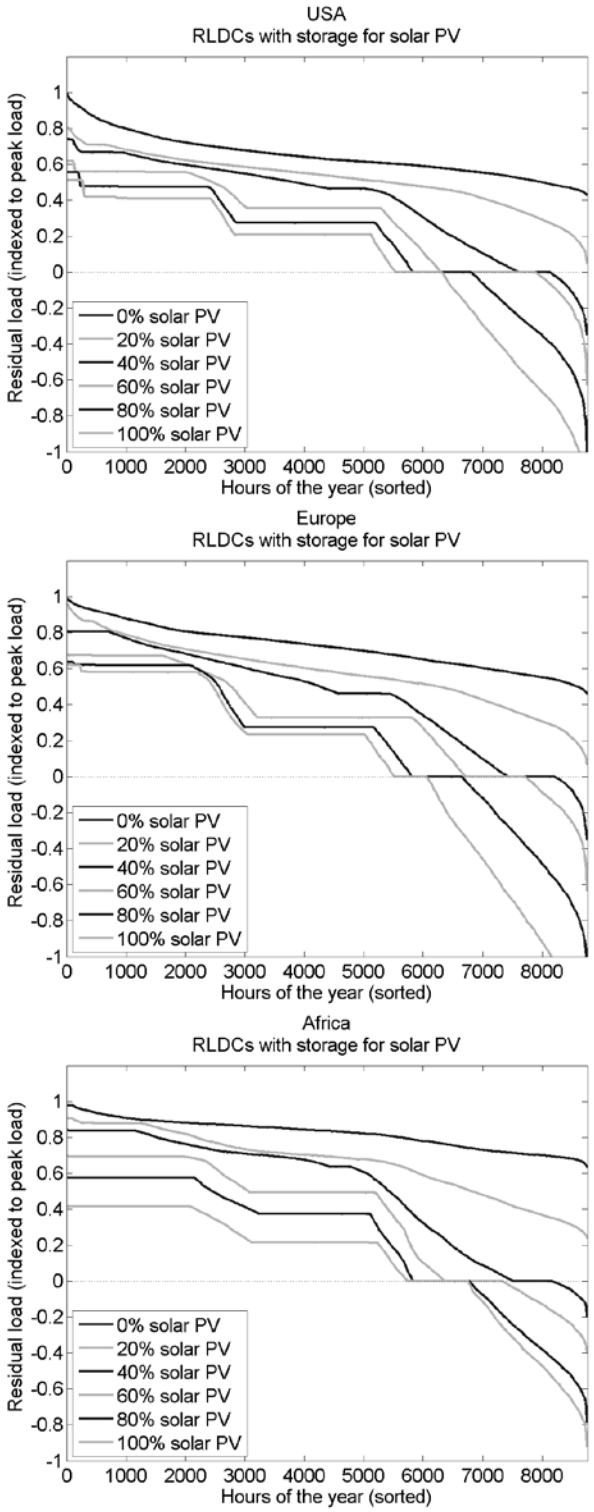


**Figure 8: RLDCs for increasing solar shares that include the impact of short-term storage estimated with the DIMES model.**

The role of short-term storage depends on both diurnal and seasonal matching of solar PV and load. Short-term storage in particular is beneficial because it distributes mid-day solar power over the day to better match load. In regions with an evening load peak like Europe and Africa, this means bridging the diurnal solar-load gap. In addition, the extent to which integration challenges can be mitigated by short-term storage depends on the seasonal matching of solar with load. For Europe short-term storage at high PV shares (~50%) is less beneficial than for Africa or the US because short-term storage cannot bridge the seasonal mismatch of European load and solar supply (Figure 8). Integration challenges can only be reduced further by long-term storage to shift electricity in seasonal scales.

Short-term storage has the highest potential of mitigating integration challenges in regions with a diurnal solar-load mismatch and a good seasonal matching, as is the case for Africa. Even though solar RLDCs without storage for Europe and Africa look very similar, with storage the picture changes such that integration challenges are much smaller in Africa. By contrast, for the US, storage has only a limited impact on solar RLDCs due to a fairly good diurnal matching during peak season even without storage. At low to moderate solar shares (<= 40%), the RLDCs hardly change because the diurnal solar peak coincides with load.

To conclude, these results indicate that determining the optimal expansion of solar PV requires a model representation of both storage (short-term and long-term) and region-specific matching properties. With short-term storage, regional differences in the RLDCs and corresponding integration challenges can increase. The seasonal correlation of VRE supply with load determines the potential role of VRE, and diurnal correlations determine if short-term storage is needed to harness this potential.

### *Curtailment and storage needs across regions*

Beyond the detailed analysis of individual RLDCs, it is also instructive to look at aggregated information from the large number of DIMES runs. In Table 3, for each region and gross VRE-share, we show curtailment values averaged across scenarios with different mixes of wind and PV given the fixed gross VRE share.

We find that under the assumptions of region-spanning transmission grids and sufficient flexible non-VRE plants, all eight analyzed world regions reach VRE shares of 40% with less than 4% curtailment, and all regions (except for India and Japan) reach VRE shares of 80% with less than 13% curtailment. Since these values are averages across all scenarios for a given VRE share, there are combinations of wind and PV that lead to higher curtailment and other combinations that lead to lower curtailment. Note that real-world curtailment rates are likely to be higher if VRE generators are deployed at a high rate (~30 percentage points per decade) and if the power system lags in adjusting to the new circumstances, e.g., by expanding transmission lines or by making dispatchable generation plants more flexible.

Table 3: Average cost-optimal curtailment (measured as share of gross VRE generation) from DIMES scenarios with storage, for all regions and VRE shares between 0-120%. Each VRE share row contains information from several scenarios, in which the mix of wind and PV was varied in steps of 10 percentage points. Accordingly, the curtailment value reported for 20%VRE is the average of the curtailment values from the 0%wind/20%PV, the 10%wind/10%PV and the 0%wind/20%PV scenario.

| Curtailment [share of VRE] | Region | | | | | | | |
|---|---|---|---|---|---|---|---|---|
| gross VRE share | AFR | CHN | EUR | IND | JPN | LAM | MEA | USA |
| 0% | 0% | 0% | 0% | 0% | 0% | 0% | 0% | 0% |
| 10% | 1% | 0% | 0% | 0% | 0% | 0% | 1% | 0% |
| 20% | 1% | 0% | 0% | 0% | 0% | 0% | 1% | 0% |
| 30% | 1% | 0% | 0% | 0% | 1% | 0% | 1% | 0% |
| 40% | 1% | 1% | 1% | 2% | 3% | 2% | 1% | 1% |
| 50% | 2% | 3% | 3% | 5% | 5% | 4% | 2% | 3% |
| 60% | 4% | 5% | 4% | 9% | 8% | 6% | 4% | 5% |
| 70% | 7% | 8% | 7% | 13% | 11% | 9% | 6% | 7% |
| 80% | 10% | 12% | 10% | 17% | 15% | 12% | 9% | 10% |
| 90% | 14% | 16% | 14% | 21% | 19% | 15% | 13% | 14% |
| 100% | 18% | 19% | 18% | 24% | 23% | 19% | 18% | 18% |
| 110% | 23% | 23% | 23% | 28% | 27% | 22% | 23% | 22% |
| 120% | 28% | 27% | 27% | 31% | 31% | 26% | 28% | 26% |

Table 4: Average cost-optimal short-term storage capacity (measured in percent of peak load) from DIMES scenarios with storage, for all regions and VRE shares between 0-120%.

| Storage capacity [% of peak load] | Region | | | | | | | |
|---|---|---|---|---|---|---|---|---|
| gross VRE share | AFR | CHN | EUR | IND | JPN | LAM | MEA | USA |
| 0% | 0% | 1% | 2% | 2% | 1% | 1% | 0% | 1% |
| 10% | 1% | 3% | 2% | 2% | 3% | 1% | 2% | 1% |
| 20% | 2% | 5% | 2% | 4% | 4% | 1% | 3% | 3% |
| 30% | 3% | 6% | 4% | 5% | 7% | 2% | 4% | 4% |
| 40% | 6% | 9% | 7% | 10% | 10% | 5% | 7% | 6% |
| 50% | 14% | 16% | 13% | 18% | 16% | 13% | 13% | 11% |
| 60% | 22% | 24% | 20% | 25% | 24% | 23% | 21% | 19% |
| 70% | 28% | 30% | 27% | 29% | 30% | 29% | 27% | 25% |
| 80% | 35% | 34% | 31% | 34% | 34% | 35% | 31% | 29% |
| 90% | 42% | 37% | 34% | 41% | 36% | 41% | 35% | 32% |
| 100% | 47% | 42% | 35% | 46% | 38% | 47% | 36% | 34% |
| 110% | 49% | 46% | 36% | 50% | 40% | 51% | 38% | 36% |
| 120% | 46% | 48% | 38% | 54% | 43% | 54% | 39% | 37% |

In Table 4, we present short-term storage capacities from the DIMES optimization. We see that in most regions, storage capacities up to 2% of peak load are cost-efficient even without any VRE. As VRE shares increase, storage capacities are deployed more, reaching on average 5-10% of peak load at 40% VRE. At 80% VRE share, the average installed storage capacity increases to 29-35% of peak load. As discussed above, the deployment of storage strongly depends on the share of PV in the system. Accordingly, the average values in the table mask that at 80% VRE share, storage capacity in wind-based scenarios

amounts to only 2-11% of peak load, while in PV-based scenarios it amounts to an impressive 50-74% of peak load.

### 3.2. Impacts of the representation of VRE integration on REMIND results

In the following, we will discuss a cost-optimal electricity sector transformation pathway, and the extent to which wind and solar technologies contribute to it. We also analyze how regional differences in technology deployment can be explained by the regional correlation of wind, solar and load as represented in the RLDCs.

Figure 9 shows global electricity production over the next century for the Tax30 scenario with stringent climate policies (30 $/tCO$_2$ tax in 2020, increasing at 5% per year, implying a >66% chance of achieving the 2°C target, more in section 2.2).

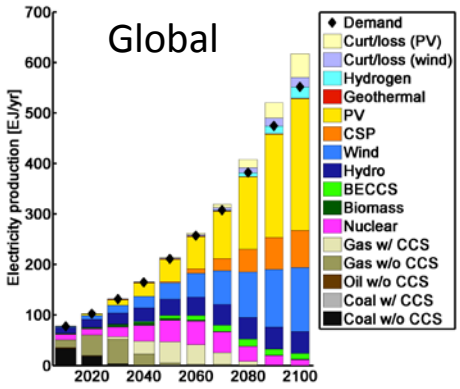


**Figure 9: Global electricity production in the Tax30 scenario. Black diamonds represent the total demand (including the electricity used for hydrogen production), with anything plotted above being curtailed.**

In the Tax30 scenario the electricity sector undergoes drastic changes: it transforms from a system based on fossil fuels to a fully decarbonized power system mostly based on renewable energy. Under our default assumptions, wind and solar are the backbone of the electricity system, with only limited contributions from hydro, nuclear, biomass, and hydrogen turbines. On a global scale, wind and solar together supply more than 70% of total electricity demand from 2070 onwards in this scenario, and 59% of the total cumulated 2010-2100 electricity demand.

VRE deployment has distinct regional patterns (see Figure 10). While the near-term deployment of new capacities in the EU has a strong focus on wind, the US deploys mostly PV over the next decades. In the long run, the development becomes similar again, with both regions deploying a mix of wind and solar, and the US also relying on concentrating solar power. Sub-Saharan Africa relies strongly on solar, with PV and CSP accounting for more than 50% of all electricity generation from 2060 onwards.

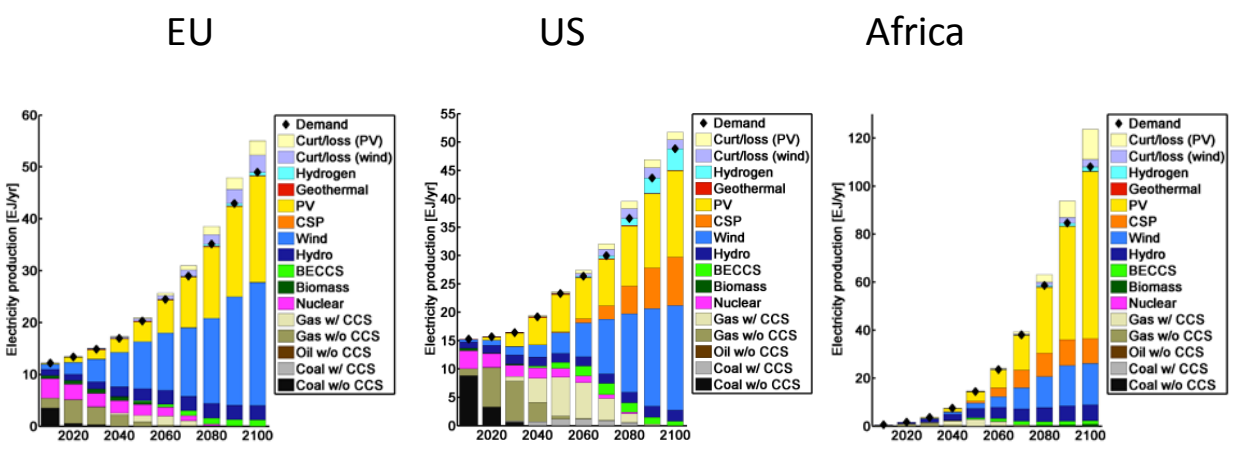


**Figure 10: Regional electricity production in the Tax30 scenario for EU (left), US (middle) and Africa (right). Black diamonds represent the total demand (including the electricity used for hydrogen production), with anything plotted above being curtailed.**

These regional differences can be explained with the regional specificities of the correlation of wind, solar, and load that we discussed above. In the US, the daily load profile in the peak season is strongly correlated with PV and thus the initial 20% of PV contribute strongly to reducing peak load even without short-term storage. As a consequence, PV generation can be integrated at low integration costs or equivalently at a high economic value. Accordingly, with the price reductions seen over the last years, PV is competitive against wind, whose generation contributes less to the more valuable peak and higher mid-load bands and more to the lower mid-load and baseload bands. In contrast, the daily load profile in the peak season in the EU is not well correlated with PV, so PV does not contribute to valuable peak load but rather mostly to base load. Wind, on the other hand, supplies a flat band in the EU for the first 20% contribution, and thereby yields a higher value per produced kWh.

As the VRE share increases and some short-term storage is built, the daily profile becomes less important, while the seasonal matching between wind, solar and load becomes more relevant. If wind and solar are seasonally anti-correlated, as is the case in both the US and the EU (see Figure 6), then the deployment of the complementary VRE technologies can improve the seasonal matching between load and VRE. Accordingly, both US and the EU tend towards a relatively even mix of solar and wind. In contrast, both solar PV and load are quite flat throughout the year in sub-Saharan Africa, so not much would be gained in terms of matching by adding wind in this case.

To better understand how such a system would operate, it is instructive to look at an illustrative example of how the resulting RLDC is met by power plants. Figure 11 shows the endogenous model RLDC for the US in 2050, for the full-technology Tax30 scenario (left) and the RE Tax30 scenario, which has the same carbon tax but does not allow deployment of nuclear and CCS in the electricity sector after 2020 (right).

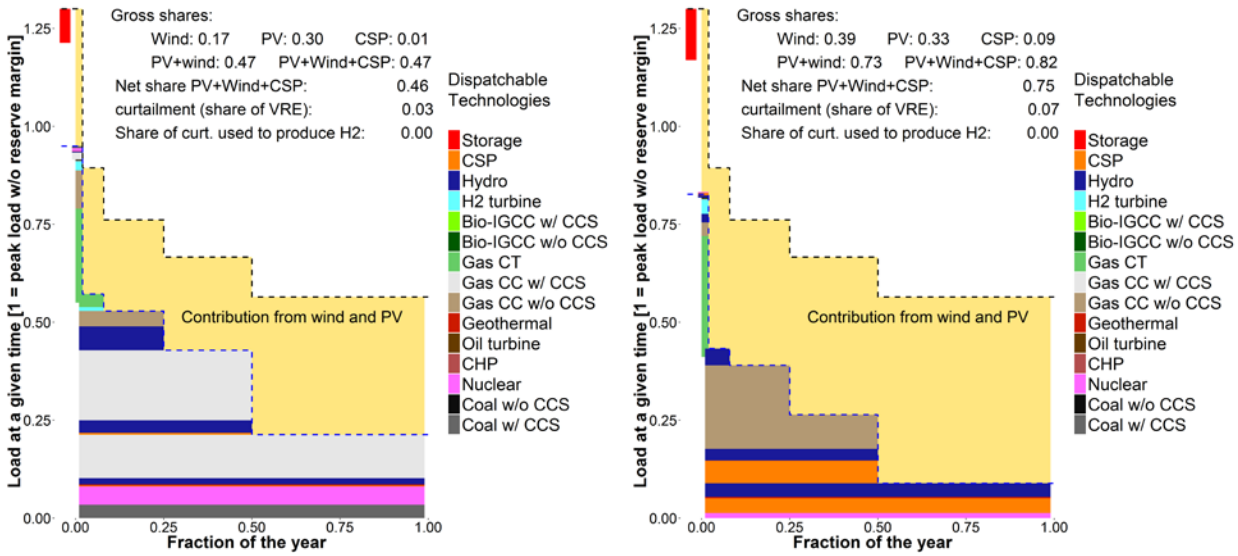


**Figure 11: Model-endogenous RLDCs for USA, 2050. Left: Tax30 scenario. Right: RE Tax30 scenario. The blue dashed line shows the residual load bands that need to be filled by dispatchable technologies, while the black dashed line represents the load bands without any VRE (LDC). The area between these two lines is the electricity supplied by wind and PV, here colored in beige, with exact shares given in the text box. Load is normalized to peak demand at 0% VRE. The model formulation requires a reserve margin of 30% on top of the peak demand as calculated from the RLDC, and assumes the plants used to cover this peak demand plus reserve margin run 1% of the year. The red bar at the top left (counting down from the 1.3 value of peak demand + reserve margin at 0% VRE) displays the size of the installed short-term storage capacity.**

In the displayed snapshot for the US in 2050 in the Tax30 scenario (Figure 11, left), wind and solar contribute to about 47% of total electricity demand, with short-term storage accounting for 5% of peak demand. The RLDC is reduced accordingly and changes shape: The baseload band decreases from ~60% of peak demand in a system without any VRE to 25%, the lower midload band roughly doubles, the upper midload stays the same, the peak load band is reduced by two thirds, and the peak demand after VRE and storage is reduced by a third. As the scenario assumes a well-developed transmission grid across the USA and also encompasses a sizeable amount of short-term storage, total curtailment is only 3% of gross VRE generation.

The RE scenario (Figure 11, right) for the US in 2050 shows a situation that seems more extreme from today's perspective: not being allowed to deploy either nuclear or CCS, the model increases the share of wind and solar to 82% of demand before curtailment, or 75% of demand after curtailment is deducted. At such high wind and solar shares, baseload is reduced to below 10% of peak demand. The remaining load bands are covered by a mix of hydro power, gas plants (both combined cycle and simple combustion turbines), and CSP. The CSP design represented in REMIND is equipped with 12h of thermal storage and can use gas or hydrogen for co-firing, which allows these CSP plants to be handled like a dispatchable power plant. The high share of wind and PV also increases the required integration measures: short-term storage is expanded to 12% of peak demand, and curtailment increases to 7% of gross VRE generation.

### *Effect on economic indicators*

The transformation of the energy system under a climate policy consistent with the 2°C target leads to electricity price increases of ~ 30% in the short term, as new capital-intensive power plants need to be constructed and old existing coal capacities are phased out before the end of their lifetime (see Figure 12). Once this transition phase is over, however, the price markup compared to a reference scenario without climate policy decreases to 10-20%. Interestingly, the scenario without nuclear and CCS in the power sector shows only a very small additional price increase compared to the Tax30 scenario.

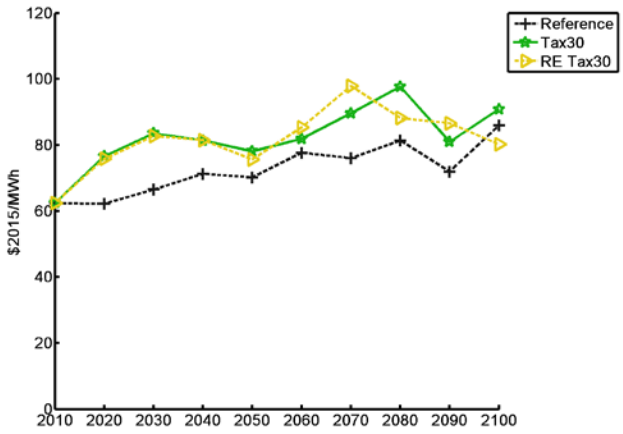


**Figure 12 : Electricity price evolution over in time in the EU in the reference scenario, the Tax30 scenario and the RE Tax30 scenario.**

From a macroeconomic perspective, the long-term mitigation costs[16] associated with reaching the 2°C target with a likelihood of >66% are about 1.87% of cumulated discounted consumption – if all technologies are available. Note that mitigation costs neither comprise the avoided impacts of climate change nor the co-benefits of mitigation. By running an additional set of scenarios where we treat wind and PV as dispatchable technologies, we can extract the influence that the detailed representation of the power sector has on mitigation costs: Explicitly representing the correlation between wind, solar and load through RLDCs increases the mitigation costs by a third from 1.4% to 1.87%. When comparing the RLDC-based model version with the previous representation of VRE in REMIND, which was based on share-dependent cost markups [28], we see that most of the variability-induced mitigation cost markup was already represented: total mitigation costs with the old implementation are 93% of the total mitigation costs with the new implementation. However, the new RLDC-based implementation has a number of striking advantages, most importantly a region-specific representation of integration challenges, a detailed representation of short-term storage and an endogenous adaptation of the non-VRE capacity mix in response to increasing VRE shares.

[16] Here measured in the reduction of consumption between the reference and the policy scenario, cumulated from 2010 to 2100 and discounted at a rate of 5%, divided by the value in the reference scenario.

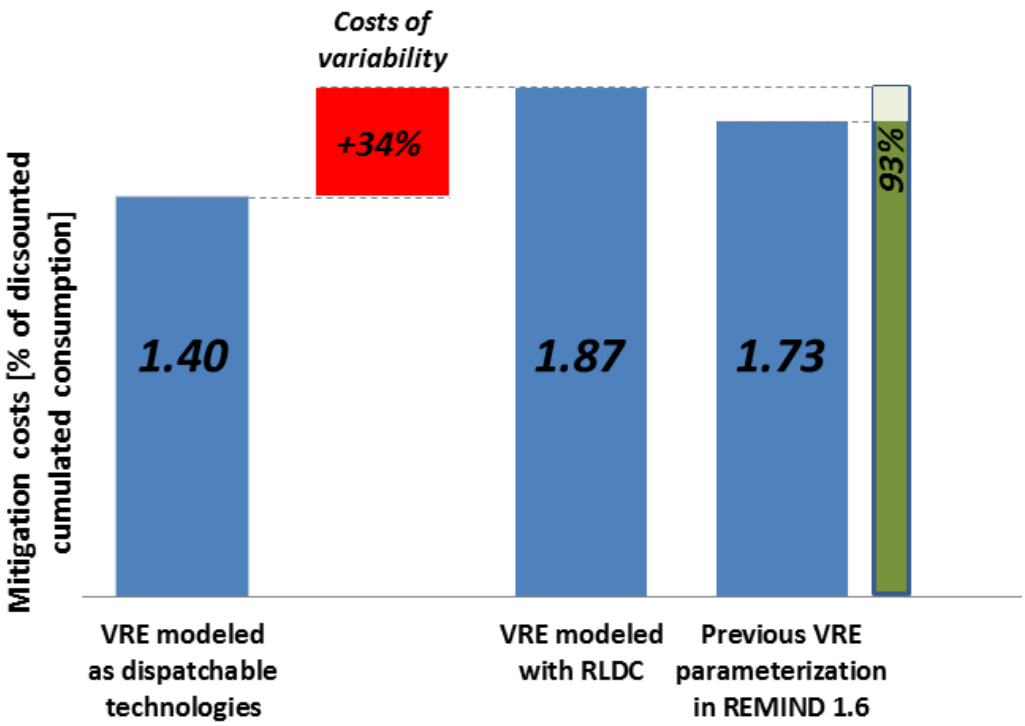


**Figure 13: Comparison of global mitigation costs between different representations of VRE variability. Mitigation costs to achieve the 2°C target with >2/3 likelihood increase by 34 percent when representing the variability of wind and solar with RLDCs as presented in this paper, compared to a counterfactual scenario where PV and wind are represented as dispatchable technologies. Most of these costs were already represented in the previous, much simpler, parameterization of variability in REMIND, which relied on share-dependent cost markups [28].**

# 4. Conclusion

As VRE generation costs decrease below those of conventional generation, in particular if meaningful $CO_2$ pricing schemes are established, integration challenges increasingly determine the role VRE have to play for power sector decarbonization. For energy-economy-climate models used for deriving long-term climate-change-mitigation scenarios, improving the representation of both VRE integration challenges and opportunities is among the highest priorities. This paper contributes three-fold to this goal:

1. It derives RLDCs that capture VRE integration challenges for eight world regions and a broad range of VRE shares and mixes. The RLDCs and underlying global VRE time series are made publicly available.
2. It explores how short-term storage changes RLDCs and mitigates region-specific integration challenges.
3. It refines the RLDC approach that allows representing major integration challenges and options in large-scale energy-economy-climate models by implementing RLDCs, and presents resulting mitigation scenarios for the REMIND model.

RLDCs capture the temporal matching of VRE supply with load, and hereby account for the most important economic impact of VRE variability. With increasing VRE generation, its load-matching becomes unfavorable, i.e., the VRE capacity credit decreases, the utilization of non-VRE power plants decreases and VRE overproduction grows. These impacts can become substantial and tend to be more costly than additional grid and balancing requirements of VRE.

We derive consistent RLDCs for eight world regions from hourly time series for wind, PV, and load, spanning a range of gross wind and PV shares from 0 to 120%. This data analysis lays the ground for moving beyond the EU/US-centeredness predominant in previous integration studies. We also estimate the impact of a cost-efficient deployment of short-term storage for the broad range of RLDCs based on DIMES, a one-node dispatch and investment model with hourly resolution. A main finding from deriving RLDCs is that if long-distance transmission grids within a region can be expanded to pool VRE supply and power demand, all eight analyzed world regions reach VRE shares of 40% with less than 4% curtailment, and all regions (except for India and Japan) reach VRE shares of 80% with less than 13% curtailment. Our results also indicate that without a representation of short-term storage (operating on diurnal time scales), the potential of solar PV tends to be underestimated.

The RLDC approach as implemented in REMIND differentiates between a broad range of wind and solar PV shares, a number of world regions, and includes the effect of potential integration measures such as storage, transmission grid investments for large area pooling (a default assumption in the REMIND model), and the adaptation of the non-VRE generation capacities in response to VRE deployment. The methodological merits allow for a greater consistency between global scenario results with detailed region-specific power sector results of partial models that are closer to engineering and planning reality. This methodological advancement is of key importance for making climate-change-mitigation scenarios more robust and credible, and hence more relevant for high-quality policy advice. In particular, the new approach allows for a more accurate estimation of the role of VRE in low-carbon transformation scenarios and mitigation costs.

Even if integration challenges are accurately accounted for, VRE play a prominent role in power sector decarbonization. For achieving the 2° target, the REMIND model shows a cost-optimal energy system transformation where wind and solar become the backbone of electricity supply. On a global scale, wind and solar together supply more than 70% of total electricity demand from 2070 onwards in this scenario. Moderate VRE shares of about 15-40% are reached in most regions by 2030 at low integration challenges if transmission grids are assumed to expand to allow regional pooling of variability. At higher VRE shares, additional VRE integration options including short-term storage, hydrogen electrolysis, and a shift in the non-VRE capacity mix towards peak plants with low specific investment costs, increasingly help to mitigate integration challenges and harness the economic potential of VRE. In addition, in regions where wind and solar are seasonally anti-correlated, an even mix of wind and solar tends to reduce integration challenges.

Achieving the 2°C target imposes mitigation costs of 1.87% of global discounted consumption from 2010-2100. In a counterfactual scenario where wind and PV are treated as dispatchable technologies, mitigation losses would decrease to 1.4%. We find that the earlier simplified modelling of variability in the REMIND versions 1.3-1.5 already represented most of the variability-induced cost markups, so that total mitigation costs with the old approach are 93% of total mitigation costs with the RLDC-based model.

While this paper provided a comprehensive description of the RLDC approach, this representation of variability is not final and should be further refined in the future. Most importantly, the data basis for deriving region-specific RLDCs should be improved in particular with regard to load data. Data gaps should be filled and the robustness should be increased by using hourly load time series and several years for all countries in each model region. Potential changes in the future load profiles and demand response should be considered. In addition, the assumption of region-spanning long-distance transmission grids should be reviewed for regions other than Europe and the US. For the time being, this paper presents a first parameterization for most world regions and thereby takes an important step towards improving the robustness of energy-economy-climate models and their representation of wind and solar around the world.

**Acknowledgements:**

The research leading to these results has received funding from the European Community's Seventh Framework Programme FP7/2012 under grant agreement n° 308329 (ADVANCE).

## 5. References

[1] REN21, “Renewables 2015 Global Status Report,” REN21 Secretariat, paris, 2015.

[2] O. Edenhofer, B. Knopf, T. Barker, L. Baumstark, E. Bellevrat, B. Chateau, P. Criqui, M. Isaac, A. Kitous, and S. Kypreos, “The economics of low stabilization: model comparison of mitigation strategies and costs,” *Energy J.*, vol. 31, no. 1, pp. 11–48, 2010.

[3] IPCC, *Special Report on Renewable Energy Sources and Climate Change Mitigation.* United Kingdom and New York, NY, USA: Cambridge University Press, 2011.

[4] V. Krey and L. Clarke, “Role of renewable energy in climate mitigation: a synthesis of recent scenarios,” *Clim. Policy*, vol. 11, no. 4, pp. 1131–1158, 2011.
[5] G. Luderer, V. Bosetti, M. Jakob, M. Leimbach, J. C. Steckel, H. Waisman, and O. Edenhofer, “The economics of decarbonizing the energy system—results and insights from the RECIPE model intercomparison,” *Clim. Change*, vol. 114, no. 1, pp. 9–37, Sep. 2012.
[6] GEA, *Global Energy Assessment - Toward a Sustainable Future*. Cambridge University Press, Cambridge, UK and New York, NY, USA and the International Institute for Applied Systems Analysis, Laxenburg, Austria, 2012.
[7] G. Luderer, V. Krey, K. Calvin, J. Merrick, S. Mima, R. Pietzcker, J. V. Vliet, and K. Wada, “The role of renewable energy in climate stabilization: results from the EMF27 scenarios,” *Clim. Change*, vol. 123, no. 3–4, pp. 427–441, Apr. 2014.
[8] O. Akashi, Y. Hijioka, T. Masui, T. Hanaoka, and M. Kainuma, “GHG emission scenarios in Asia and the world: The key technologies for significant reduction,” *Energy Econ.*, vol. 34, pp. S346–S358, Dec. 2012.
[9] A. Mills and R. Wiser, “Changes in the Economic Value of Variable Generation at High Penetration Levels: A Pilot Case Study of California.” Ernest Orlando Lawrence Berkeley National Laboratory, 2012.
[10] F. Ueckerdt, L. Hirth, G. Luderer, and O. Edenhofer, “System LCOE: What are the costs of variable renewables?,” *Energy*, vol. 63, pp. 61–75, Dec. 2013.
[11] L. Hirth, “The market value of variable renewables: The effect of solar wind power variability on their relative price,” *Energy Econ.*, vol. 38, pp. 218–236, Jul. 2013.
[12] IEA, “The Power of Transformation - Wind, Sun and the Economics of Flexible Power Systems,” IEA/OECD, Paris, 2014.
[13] L. Hirth, F. Ueckerdt, and O. Edenhofer, “Integration costs revisited – An economic framework for wind and solar variability,” *Renew. Energy*, vol. 74, pp. 925–939, Feb. 2015.
[14] A. S. Brouwer, M. van den Broek, W. Zappa, W. C. Turkenburg, and A. Faaij, “Least-cost options for integrating intermittent renewables in low-carbon power systems,” *Appl. Energy*, vol. 161, pp. 48–74, Jan. 2016.
[15] F. Ueckerdt, R. Brecha, G. Luderer, P. Sullivan, E. Schmid, N. Bauer, D. Böttger, and R. Pietzcker, “Representing power sector variability and the integration of variable renewables in long-term energy-economy models using residual load duration curves,” *Energy*, Jul. 2015.
[16] G. Blanford, R. Aalbers, J. Bollen, and K. Folmer, “Technological Uncertainty in Meeting Europe’s Decarbonisation Goals.” CPB Discussion Paper, 2015.
[17] F. Ueckerdt, R. Brecha, and G. Luderer, “Analyzing major challenges of wind and solar variability in power systems,” *Renew. Energy*, vol. 81, pp. 1–10, Sep. 2015.
[18] R. C. Pietzcker, F. Ueckerdt, S. Carrara, H.-S. De Boer, J. Després, S. Fujimori, N. Johnson, A. Kitous, Y. Scholz, P. Sullivan, and G. Luderer, “Evaluating the capacity of Integrated Assessment Models to represent system integration challenges of wind and solar power,” *Energy Econ. Submitt.*, no. this issue.
[19] G. Luderer, R. C. Pietzcker, S. Carrara, H.-S. De Boer, S. Fujimori, N. Johnson, S. Mima, and D. Arent, “Renewable Energy Futures: An overview of results from the ADVANCE project,” *Energy Econ. Submitt.*, no. this issue.
[20] Global Energy System Modeling Group and Potsdam Institute for Climate Impact Research, “REMIND Documentation,” 2013. [Online]. Available: http://www.pik-potsdam.de/research/sustainable-solutions/models/remind/description-of-remind-v1.5.
[21] N. Bauer, R. J. Brecha, and G. Luderer, “Economics of nuclear power and climate change mitigation policies,” *Proc. Natl. Acad. Sci.*, vol. 109, no. 42, pp. 16805–16810, Oct. 2012.

[22] M. Leimbach, N. Bauer, L. Baumstark, M. Luken, and O. Edenhofer, “Technological Change and International Trade - Insights from REMIND-R,” *Energy J.*, vol. 31, no. Special Issue, pp. 109–136, 2010.
[23] G. Luderer, R. C. Pietzcker, C. Bertram, E. Kriegler, M. Meinshausen, and O. Edenhofer, “Economic mitigation challenges: how further delay closes the door for achieving climate targets,” *Environ. Res. Lett.*, vol. 8, no. 3, p. 034033, Sep. 2013.
[24] M. Fürsch, S. Hagspiel, C. Jägemann, S. Nagl, D. Lindenberger, and E. Tröster, “The role of grid extensions in a cost-efficient transformation of the European electricity system until 2050,” *Appl. Energy*, vol. 104, pp. 642–652, Apr. 2013.
[25] S. Becker, R. A. Rodriguez, G. B. Andresen, S. Schramm, and M. Greiner, “Transmission grid extensions during the build-up of a fully renewable pan-European electricity supply,” *Energy*, vol. 64, pp. 404–418, Jan. 2014.
[26] K. Schaber, F. Steinke, and T. Hamacher, “Transmission grid extensions for the integration of variable renewable energies in Europe: Who benefits where?,” *Energy Policy*, vol. 43, pp. 123–135, Apr. 2012.
[27] M. Haller, S. Ludig, and N. Bauer, “Decarbonization scenarios for the EU and MENA power system: Considering spatial distribution and short term dynamics of renewable generation,” *Energy Policy*, vol. 47, no. C, pp. 282–290, 2012.
[28] R. C. Pietzcker, D. Stetter, S. Manger, and G. Luderer, “Using the sun to decarbonize the power sector: The economic potential of photovoltaics and concentrating solar power,” *Appl. Energy*, vol. 135, pp. 704–720, Dec. 2014.
[29] Y. Scholz, H.-C. Gils, and R. C. Pietzcker, “Application of a high-detail energy system model to derive power sector characteristics at high wind and solar shares,” *Energy Econ. Submitt.*, 2016.
[30] C. Bertram, G. Luderer, R. C. Pietzcker, E. Schmid, E. Kriegler, and O. Edenhofer, “Complementing carbon prices with technology policies to keep climate targets within reach,” *Nat. Clim. Change*, vol. 5, no. 3, pp. 235–239, Mar. 2015.
[31] C. Paul, “Bilanzierungsmodell zur Bestimmung der regenerativen Stromüberschüsse der MENA-Region im Jahr 2050,” University of Stuttgart, 2007.
[32] W. Chen, F. Zhou, X. Han, and B. Shan, “Analysis on Load Characteristics of State Grid,” *Electr. Power Technol. Econ.*, vol. 37, no. 4, pp. 25–29, 2008.
[33] G. He and D. M. Kammen, “Where, when and how much wind is available? A provincial-scale wind resource assessment for China,” *Energy Policy*, vol. 74, pp. 116–122, Nov. 2014.
[34] Z. Hu, X. Tan, and Z. Xu, *An exploration into China’s economic development and electricity demand by the year 2050*. London ; Waltham, MA: Elsevier, 2014.
[35] D. Stetter, “Enhancement of the REMix energy model – global renewable energy potentials optimized power plant siting and scenario validation,” PhD Thesis, University of Stuttgart, 2012.
[36] E. Bartholomé and A. S. Belward, “GLC2000: a new approach to global land cover mapping from Earth observation data,” *Int. J. Remote Sens.*, vol. 26, no. 9, pp. 1959–1977, May 2005.
[37] National Aeronautics and Space Agency NASA, “Surface Radiation Budget Release 3.0,” Atmospheric Science Data Center, 2012.
[38] National Aeronautics and Space Agency NASA, “Modern Era Retrospective-analysis for Research and Applications MERRA,” Modeling and Assimilation Data and Information Services Center, 2012.
[39] Y. Scholz, “Renewable energy based electricity supply at low costs: development of the REMix model and application for Europe,” University of Stuttgart, 2012.
[40] J. P. Deane, A. Chiodi, M. Gargiulo, and B. P. Ó Gallachóir, “Soft-linking of a power systems model to an energy systems model,” *Energy*, vol. 42, no. 1, pp. 303–312, Jun. 2012.
[41] NREL, “Renewable Electricity Futures Study,” National Renewable Energy Laboratory, Golden, CO, 2012.

[42] M. Chaudry, P. Ekins, K. Ramachandran, A. Shakoor, J. Skea, G. Strbac, X. Wang, and J. Whitaker, "Building a resilient UK energy system," 2011.
[43] H. Holttinen, P. Meibom, A. Orths, B. Lange, M. O'Malley, J. O. Tande, A. Estanqueiro, E. Gomez, L. Söder, G. Strbac, J. C. Smith, and F. van Hulle, "Impacts of large amounts of wind power on design and operation of power systems, results of IEA collaboration," *Wind Energy*, vol. 14, no. 2, pp. 179–192, 2011.
[44] DIG SILENT and Ecofys, "All Island TSO Faciliation Of Renewables Studies," 2010.
[45] EirGrid/SONI, "DS3 Programme - Operational Capability Outlook 2015." 2015.
[46] E. Ela, V. Gevorgian, P. Fleming, Y. C. Zhang, M. Singh, E. Muljadi, A. Scholbrook, J. Aho, A. Buckspan, L. Pao, V. Singhvi, A. Tuohy, P. Pourbeik, D. Brooks, and N. Bhatt, "Active Power Controls from Wind Power: Bridging the Gaps," NREL, Technical Report NREL/TP-5D00-60574, 2014.
[47] M. Z. Jacobson, M. A. Delucchi, M. A. Cameron, and B. A. Frew, "Low-cost solution to the grid reliability problem with 100% penetration of intermittent wind, water, and solar for all purposes," *Proc. Natl. Acad. Sci.*, vol. 112, no. 49, pp. 15060–15065, Dec. 2015.
[48] T. Boßmann and I. Staffell, "The shape of future electricity demand: Exploring load curves in 2050s Germany and Britain," *Energy*, vol. 90, pp. 1317–1333, Oct. 2015.
[49] F. M. Andersen, H. V. Larsen, and T. K. Boomsma, "Long-term forecasting of hourly electricity load: Identification of consumption profiles and segmentation of customers," *Energy Convers. Manag.*, vol. 68, pp. 244–252, Apr. 2013.
[50] K. Qian, C. Zhou, M. Allan, and Y. Yuan, "Modeling of Load Demand Due to EV Battery Charging in Distribution Systems," *IEEE Trans. Power Syst.*, vol. 26, no. 2, pp. 802–810, May 2011.
[51] P. Sullivan, V. Krey, and K. Riahi, "Impacts of considering electric sector variability and reliability in the MESSAGE model," *Energy Strategy Rev.*, vol. 1, no. 3, pp. 157–163, Mar. 2013.

# A. Appendix

## A.1. Polynomial coefficients

In section 2.5 we report that six parameters control the changes of the implemented RLDCs with increasing wind and solar PV shares. These parameters are residual peak load $H_P$, the curtailment rate $\gamma$ and four cumulative heights $H_{1..4}$ of the load bands that build the stepwise RLDC approximation (Figure 14).

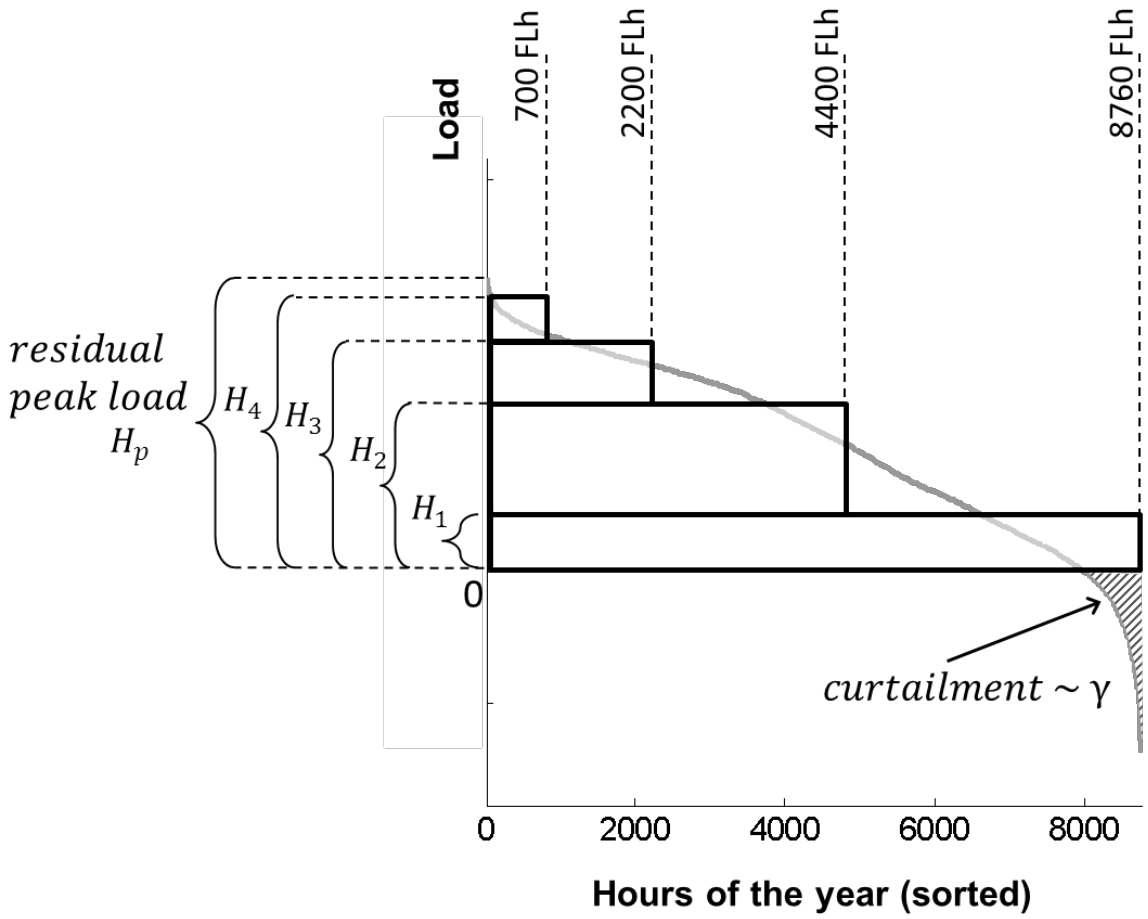


**Figure 14: The RLDC model representation is controlled by six parameters: four cumulative heights $H_{1..4}$ of the load bands, residual peak load $H_P$ and the curtailment rate $\gamma$.**

In addition, two more parameters are endogenously determined in DIMES for all VRE shares and mixes and then made an exogenous input to the REMIND model: short-term storage capacity and corresponding storage costs.

Each of the eight parameters is controlled by a third-degree polynomial function $F(\alpha, \beta)$ depending on wind and PV share of the form shown in equation (1) where $\alpha$ and $\beta$ are the wind and solar share and $a_{xx}$ the polynomial coefficients. $\alpha$ and $\beta$ are given in units of total load, i.e., if $\alpha = 1$ annual wind generation equals annual load. These shares are calculated before curtailment, which is why $\alpha$ and $\beta$ do not necessarily equal the final VRE share in consumption and might be higher than 1.

$$F(\alpha,\beta) = a_{00} + a_{10}\alpha + a_{01}\beta + a_{20}\alpha^2 + a_{02}\beta^2 + a_{11}\alpha\beta + a_{21}\alpha^2\beta + a_{12}\alpha\beta^2 + a_{30}\alpha^3 + a_{03}\beta^3 \quad (1)$$

Table 5 shows the coefficients for all seven parameters and eight REMIND model regions. The remaining three REMIND model regions have no specific parameterization but are approximated with the same coefficients as related model regions (Europe is used as a proxy for Russia, India for Other Asia, USA for Rest Of the World).

**Table 5 : Coefficients of polynomial functions that determine seven parameters for REMIND model regions.**

| | | Parameter | | | | | | | |
|---|---|---|---|---|---|---|---|---|---|
| | | **Curtail-ment rate $\gamma$** | **Short-term storage capacity** | **Short-term storage cost** | **Height load band $H_1$** | **Height load band $H_2$** | **Height load band $H_3$** | **Height load band $H_4$** | **Residual peak load $H_p$** |
| | | Share of VRE generation | Share of peak load | $ per W of peak load | Normalized such that the sum of the four RLDC boxes is the share of total load that needs to be covered by non-VRE generation (i.e. 1 for no VRE) | | | | |
| Europe | $a_{00}$ | 0.000 | 0.000 | 0.000 | 1.301 | 1.175 | 1.058 | 0.871 | 1.386 |
| | $a_{10}$ | 0.048 | 0.000 | 0.000 | -1.066 | -1.189 | -1.013 | -1.138 | -0.588 |
| | $a_{01}$ | 0.017 | 0.000 | 0.000 | -0.467 | -0.806 | -0.756 | -1.729 | -0.483 |
| | $a_{20}$ | -0.220 | 0.039 | 0.038 | 0.602 | 0.783 | 0.124 | 0.064 | 0.013 |
| | $a_{11}$ | -0.191 | 0.513 | -0.008 | -0.585 | 0.402 | -0.588 | 1.359 | -0.662 |
| | $a_{02}$ | -0.046 | 1.435 | 1.157 | -0.171 | 1.013 | 0.004 | 1.135 | -0.397 |
| | $a_{30}$ | 0.336 | -0.020 | -0.018 | -0.172 | -0.302 | 0.024 | 0.151 | 0.079 |
| | $a_{21}$ | 0.556 | 0.000 | 0.163 | -0.223 | -0.993 | 0.341 | -0.281 | 0.000 |
| | $a_{12}$ | 0.191 | -0.197 | 0.731 | 0.346 | -0.657 | 0.108 | -0.476 | 0.255 |
| | $a_{03}$ | 0.309 | -0.736 | -0.593 | 0.158 | -0.578 | 0.112 | -0.244 | 0.299 |
| | $R^2$ | 0.935 | 0.842 | 0.923 | 0.991 | 0.993 | 0.991 | 0.979 | 0.964 |
| Latin America | $a_{00}$ | 0.000 | 0.000 | 0.000 | 1.224 | 1.160 | 1.080 | 0.875 | 1.312 |
| | $a_{10}$ | 0.005 | 0.000 | 0.000 | -0.707 | -0.962 | -1.014 | -1.308 | -0.627 |
| | $a_{01}$ | 0.002 | 0.000 | 0.000 | -0.142 | -0.219 | -0.712 | -1.893 | -0.377 |
| | $a_{20}$ | -0.064 | 0.106 | 0.026 | 0.094 | 0.530 | 0.260 | 0.367 | 0.286 |
| | $a_{11}$ | -0.059 | 0.642 | 0.599 | -1.118 | -0.615 | -0.822 | 1.703 | -0.678 |
| | $a_{02}$ | 0.112 | 1.293 | 0.743 | -0.615 | -0.316 | 0.106 | 1.441 | -0.594 |
| | $a_{30}$ | 0.247 | 0.003 | 0.059 | 0.018 | -0.257 | -0.096 | 0.041 | -0.133 |
| | $a_{21}$ | 0.393 | -0.379 | -0.283 | 0.252 | -0.261 | 0.346 | -0.418 | 0.293 |
| | $a_{12}$ | 0.159 | 0.109 | 0.403 | 0.576 | 0.438 | 0.429 | -0.638 | 0.265 |
| | $a_{03}$ | 0.062 | -0.366 | 0.143 | 0.162 | -0.023 | -0.140 | -0.367 | 0.278 |
| | $R^2$ | 0.892 | 0.958 | 0.968 | 0.991 | 0.996 | 0.994 | 0.986 | 0.978 |

| | | | | | | | | | |
|---|---|---|---|---|---|---|---|---|---|
| India | $a_{00}$ | 0.000 | 0.000 | 0.000 | 1.111 | 1.060 | 1.020 | 0.960 | 1.182 |
| | $a_{10}$ | 0.002 | 0.059 | 0.016 | -0.614 | -0.685 | -0.872 | -1.749 | -0.517 |
| | $a_{01}$ | 0.002 | 0.000 | 0.000 | -0.064 | -0.085 | -0.382 | -2.195 | -0.127 |
| | $a_{20}$ | 0.190 | -0.056 | -0.011 | 0.616 | 0.665 | 0.705 | 1.020 | 0.484 |
| | $a_{11}$ | -0.052 | 0.368 | 0.493 | -0.808 | -1.068 | -1.165 | 2.389 | -0.296 |
| | $a_{02}$ | 0.052 | 1.779 | 1.008 | -0.574 | -0.323 | -0.117 | 1.791 | -0.833 |
| | $a_{30}$ | 0.150 | 0.018 | 0.002 | -0.292 | -0.357 | -0.373 | -0.205 | -0.195 |
| | $a_{21}$ | 0.306 | 0.024 | -0.085 | 0.016 | -0.045 | -0.020 | -0.636 | -0.140 |
| | $a_{12}$ | 0.301 | -0.311 | -0.209 | 0.611 | 0.836 | 0.836 | -1.001 | 0.348 |
| | $a_{03}$ | 0.161 | -0.807 | -0.051 | 0.102 | -0.086 | -0.116 | -0.487 | 0.343 |
| | $R^2$ | 0.835 | 0.939 | 0.964 | 0.974 | 0.986 | 0.992 | 0.988 | 0.977 |
| USA | $a_{00}$ | 0.000 | 0.000 | 0.000 | 1.381 | 1.176 | 1.029 | 0.872 | 1.544 |
| | $a_{10}$ | 0.018 | 0.001 | 0.000 | -0.838 | -0.949 | -0.957 | -1.280 | -0.687 |
| | $a_{01}$ | 0.006 | 0.000 | 0.000 | -1.558 | -0.881 | -0.555 | -1.601 | -1.934 |
| | $a_{20}$ | -0.119 | 0.029 | 0.036 | 0.492 | 0.420 | 0.100 | 0.238 | 0.330 |
| | $a_{11}$ | -0.112 | 0.490 | 0.235 | -1.032 | -0.190 | -0.644 | 1.588 | -0.822 |
| | $a_{02}$ | 0.052 | 1.314 | 0.819 | 1.853 | 0.924 | -0.219 | 0.915 | 2.325 |
| | $a_{30}$ | 0.263 | 0.026 | -0.012 | -0.257 | -0.206 | -0.001 | 0.109 | -0.186 |
| | $a_{21}$ | 0.532 | -0.314 | -0.181 | 0.477 | -0.084 | 0.358 | -0.425 | 0.317 |
| | $a_{12}$ | 0.175 | 0.128 | 0.506 | 0.351 | -0.287 | 0.195 | -0.527 | 0.454 |
| | $a_{03}$ | 0.153 | -0.674 | -0.233 | -0.963 | -0.574 | 0.138 | -0.159 | -1.148 |
| | $R^2$ | 0.953 | 0.911 | 0.935 | 0.989 | 0.993 | 0.994 | 0.983 | 0.975 |
| Japan | $a_{00}$ | 0.000 | 0.000 | 0.000 | 1.275 | 1.147 | 1.045 | 0.891 | 1.429 |
| | $a_{10}$ | 0.001 | 0.000 | 0.000 | -0.802 | -0.985 | -1.030 | -1.462 | -0.514 |
| | $a_{01}$ | 0.000 | 0.226 | 0.000 | -0.719 | -0.419 | -0.565 | -1.813 | -1.172 |
| | $a_{20}$ | -0.036 | 0.067 | 0.037 | 0.592 | 0.856 | 0.633 | 0.607 | 0.337 |
| | $a_{11}$ | -0.007 | 0.800 | 0.853 | -1.065 | -0.622 | -0.797 | 1.854 | -1.125 |
| | $a_{02}$ | 0.280 | 0.971 | 1.225 | 0.369 | 0.143 | 0.040 | 1.309 | 0.901 |
| | $a_{30}$ | 0.330 | -0.034 | -0.014 | -0.236 | -0.397 | -0.311 | -0.051 | -0.121 |
| | $a_{21}$ | 0.135 | 0.000 | 0.000 | 0.395 | -0.163 | 0.031 | -0.474 | 0.093 |
| | $a_{12}$ | 0.009 | -0.308 | -0.328 | 0.302 | 0.053 | 0.259 | -0.670 | 0.471 |
| | $a_{03}$ | 0.041 | -0.542 | -0.628 | -0.107 | -0.093 | 0.033 | -0.315 | -0.287 |
| | $R^2$ | 0.910 | 0.867 | 0.926 | 0.993 | 0.995 | 0.997 | 0.983 | 0.986 |

| | | | | | | | | | |
|---|---|---|---|---|---|---|---|---|---|
| Middle East North Africa | $a_{00}$ | 0.000 | 0.000 | 0.000 | 1.217 | 1.154 | 1.073 | 0.885 | 1.283 |
| | $a_{10}$ | 0.050 | 0.084 | 0.010 | -0.997 | -1.058 | -1.045 | -1.133 | -0.795 |
| | $a_{01}$ | 0.050 | 0.000 | 0.000 | -0.136 | -0.387 | -1.202 | -1.779 | -0.312 |
| | $a_{20}$ | -0.185 | -0.125 | 0.003 | 0.362 | 0.252 | 0.113 | 0.066 | 0.231 |
| | $a_{11}$ | -0.351 | 0.409 | 0.339 | -0.530 | -0.661 | -0.293 | 1.542 | -0.436 |
| | $a_{02}$ | -0.206 | 1.571 | 0.930 | -0.807 | -0.276 | 1.335 | 1.189 | -0.743 |
| | $a_{30}$ | 0.229 | 0.062 | 0.009 | -0.109 | -0.055 | -0.004 | 0.136 | -0.039 |
| | $a_{21}$ | 0.650 | -0.133 | -0.185 | -0.296 | -0.118 | 0.304 | -0.294 | 0.000 |
| | $a_{12}$ | 0.621 | -0.091 | 0.083 | 0.448 | 0.553 | 0.073 | -0.561 | 0.168 |
| | $a_{03}$ | 0.367 | -0.806 | -0.227 | 0.374 | 0.058 | -0.799 | -0.260 | 0.442 |
| | $R^2$ | 0.872 | 0.907 | 0.943 | 0.989 | 0.989 | 0.991 | 0.983 | 0.969 |
| Sub-Saharan Africa | $a_{00}$ | 0.000 | 0.000 | 0.000 | 1.165 | 1.093 | 1.043 | 0.929 | 1.225 |
| | $a_{10}$ | 0.050 | 0.023 | 0.000 | -0.977 | -0.979 | -1.065 | -1.206 | -0.977 |
| | $a_{01}$ | 0.044 | 0.000 | 0.000 | 0.000 | -0.137 | -0.703 | -2.062 | -0.084 |
| | $a_{20}$ | -0.196 | -0.031 | 0.038 | 0.409 | 0.284 | 0.265 | 0.100 | 0.742 |
| | $a_{11}$ | -0.344 | 0.547 | 0.384 | -0.714 | -0.814 | -0.592 | 1.817 | -0.426 |
| | $a_{02}$ | -0.141 | 1.619 | 0.803 | -0.827 | -0.426 | 0.344 | 1.557 | -0.985 |
| | $a_{30}$ | 0.258 | 0.014 | -0.018 | -0.106 | -0.077 | -0.096 | 0.143 | -0.273 |
| | $a_{21}$ | 0.681 | -0.019 | -0.184 | -0.058 | -0.084 | 0.206 | -0.399 | -0.294 |
| | $a_{12}$ | 0.598 | -0.392 | 0.239 | 0.586 | 0.713 | 0.555 | -0.688 | 0.478 |
| | $a_{03}$ | 0.266 | -0.579 | 0.172 | 0.236 | 0.007 | -0.336 | -0.392 | 0.410 |
| | $R^2$ | 0.846 | 0.936 | 0.940 | 0.986 | 0.991 | 0.988 | 0.983 | 0.976 |
| China | $a_{00}$ | 0.000 | 0.000 | 0.000 | 1.176 | 1.131 | 1.037 | 0.908 | 1.201 |
| | $a_{10}$ | 0.008 | 0.109 | 0.000 | -0.778 | -0.921 | -0.855 | -1.039 | -0.447 |
| | $a_{01}$ | 0.004 | 0.000 | 0.000 | -0.470 | -0.658 | -0.629 | -1.881 | -0.550 |
| | $a_{20}$ | -0.073 | -0.060 | 0.067 | 0.205 | 0.313 | -0.045 | -0.157 | 0.055 |
| | $a_{11}$ | -0.087 | 0.588 | 0.725 | -0.674 | -0.052 | -0.757 | 1.434 | -0.875 |
| | $a_{02}$ | 0.073 | 1.571 | 1.093 | 0.019 | 0.680 | 0.239 | 1.282 | 0.076 |
| | $a_{30}$ | 0.211 | 0.009 | -0.034 | -0.034 | -0.133 | 0.054 | 0.233 | -0.007 |
| | $a_{21}$ | 0.426 | 0.000 | -0.177 | -0.107 | -0.412 | 0.259 | -0.273 | 0.189 |
| | $a_{12}$ | 0.252 | -0.226 | -0.066 | 0.471 | -0.200 | 0.349 | -0.489 | 0.339 |
| | $a_{03}$ | 0.191 | -0.806 | -0.434 | -0.023 | -0.491 | -0.174 | -0.291 | 0.005 |
| | $R^2$ | 0.883 | 0.903 | 0.946 | 0.991 | 0.994 | 0.996 | 0.985 | 0.982 |

## A.2. Equations of the RLDC approach

In the following we show the core equations of representing RLDCs in the REMIND model. All equations are valid for each time step, i.e., every variable also depends on the time step, which is not written out

here for better readability. Figure 15 illustrates the stepwise RLDC approximation in REMIND and indicates core variables.

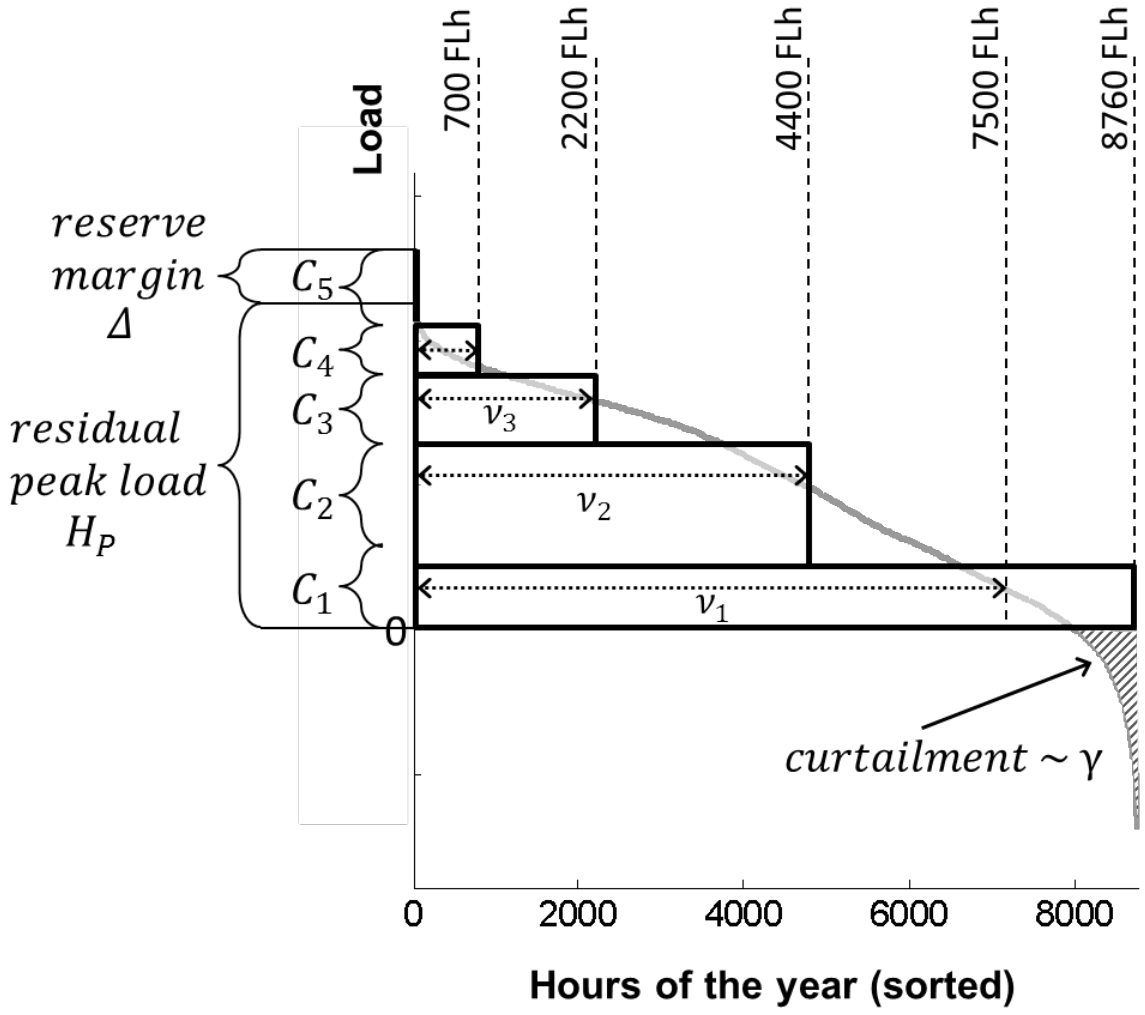


**Figure 15: Key variables representing the RLDCs in the model are the individual heights of four load bands $C_1..C_4$, reserve capacity $C_5$ (peak capacity + reserve margin $\Delta$) and curtailment rate $\alpha$. The widths of the bands $v_i$ are constant and determine the FLH of non-VRE plants that cover this part of load. Non-VRE plants operating in the base-load band have an adjusted capacity factor of 7500 annual operating hours.**

From the cumulate height $H_i$ of the four load bands i determined by a polynomial function as described in A.1, the height of the individual load bands $C_i$ is calculated according to:

$$C_i = max(H_i, 0) - \max(H_{i-1}, 0) \qquad for\ i = 1..4 \qquad (2)$$

The max() function is used here because the polynomial fit function of $H_i$ can become negative at the boundaries of the parameter space, i.e. at very high shares of VRE when RLDCs become very flat and e.g. the base-load band vanishes. Negative fit values are allowed for to increase the accuracy of the fit within the relevant positive parameter space at lower VRE shares, e.g. when the base-load band did not yet

vanish. Constraining the fit functions to only positive values would require higher polynomial orders to capture the asymptotic behaviour of some parameters e.g. the base-load height approaches zero quickly with increasing VRE share.

$C_i$ capture the shape of the load-band representation of the RLDC, which is region-specific and changes with VRE share and mix. Reserve capacity $C_5$ consists of peak capacity, which is capacity that operates only a few hours per year to cover residual peak load, and a capacity margin $\Delta$. The capacity margin provides additional firm capacity to assure reliability in case of contingency events, e.g. outages of plants or grid connections. The specific margin depends on region-dependent industry standards. We apply a reserve margin of 30% of peak load.

The load bands have to be filled by dispatchable technologies. Thus, for every non-VRE power generating technology $te$ the respective total installed capacity $C_{tot,te}$ is endogenously decomposed into five parts ($C_{1,te}$, $C_{2,te}$, $C_{3,te}$, $C_{4,te}$, $C_{5,te}$) that operate in the four load bands or act as reserve capacity.

$$C_{tot,te} = \sum_{i=1..5} C_{i,te} \tag{3}$$

When adding all the capacity over all non-VRE technologies that operate in a specific load band, this should equal the total capacity demand $C_i$ for this load band (equation 4). In the base-load band the maximum number of FLH of generators is limited to 7500 per year to account for plant outages. Hence, some more base-load capacity needs to be allocated than the parameterized height $C_1$ indicates (equation 5).

$$C_i = \sum_{te} C_{i,te} \qquad for\ i = 2..4 \tag{4}$$

$$C_1 = \frac{7500h}{8760h} \sum_{te} C_{1,te} \qquad for\ i = 1 \tag{5}$$

Additionally, there is a capacity adequacy equation that

The total peak capacity requirements are represented in a single model equation (similar to [15], [51]), which requires that the sum of all non-VRE capacities is larger than the residual peak load $H_P$ (at a given wind and PV share) plus the capacity reserve margin $\Delta$, which is described above.

$$H_P + \Delta \leq \sum_{te} C_{tot,te} \tag{6}$$

The annual capacity factor of any generation unit equals the width $v_i$ of the respective load band in which the unit operates and is in principle independent of the specific technology $te$. Planned outages of power plants are assumed to be conducted in the "$1 - v$" part of the year, i.e., while the plants are not needed. Unplanned outages are compensated by the additional reserve capacity margin.

The balance equation for total annual demand $D$ and generation is given by:

$$D = \sum_{i} \sum_{te} C_{i,te} v_i + (1 - \gamma) G_{vre} \tag{7}$$

The first summand is the generation of all non-VRE technologies $te$. The second summand is the part of VRE generation $G_{vre}$ that can be used to cover demand. $\gamma$ is the curtailment rate of VRE generation, which is also parameterized by polynomial functions depending on the endogenous share and mix of VRE.

For some technologies, additional restrictions apply:

- Combined heat and power plants have a maximum total capacity factor of 0.6 to represent that there is not always demand for heat.
- Hydro power is only counted with 80% towards the capacity adequacy equation to represent that some part of run-of-river hydro cannot contribute to meet peak demand.
- CSP is treated as a dispatchable technology, but requires a certain amount of either gas or hydrogen for co-firing. This amount increases as
    1. CSP is dispatched into the base-load band or lower mid-load band
    2. The share of CSP in the total generation increases
    3. The share of PV in the total generation increases
    4. CSP is used in a region with suboptimal resources
- Hydrogen storage : The model can invest into two types of electrolysis, one a dedicated electrolysis plant that is run at a capacity factor of 90%, and accordingly increases load, the other one a flexible electrolysis plant that uses curtailed electricity to produce hydrogen. Accordingly, it runs at low capacity factors that endogenously depend on the amount of curtailment - the higher the curtailment, the higher the capacity factor of the electrolysis plant.

## A.3. Variation of grid costs

As discussed in section 2.3 and 2.6, the model scope of REMIND makes a detailed representation of transmission grids impossible. Instead, the model relies on an aggregated representation of grid costs through two channels: i) all electricity use requires investment into a general transmission and distribution grid, which results in grid costs of 25-30$/MWh, ii) an additional cost markup on all electricity production from VRE represents the requirement to expand the transmission grid to pool variability over large areas. This second component was fitted to the results from the detailed hourly power sector model REMix, which represents 16 EU member states and endogenously models cost-optimal grid expansion [29]. For the EU, these cost markups amount to 6-11$/MWh VRE, while for larger regions like China, AFR or LAM we double these costs to 13-23$/MWh VRE. From the range of published grid costs numbers (see [13] for a literature review of VRE-related grid costs) we think that these assumptions are a reasonable starting point, but again, most of the previous modelling results focus on US and EU, so much better disaggregated modelling for other world regions is required to improve the knowledge about region-specific grid expansion costs.

To test the impact of the grid cost assumptions on the deployment of VRE, we ran sensitivity scenarios where we increased/decreased the VRE-related grid costs for all regions by a constant factor. Figure 16

shows that doubling the grid costs reduces the contribution of VRE to total electricity production by 13%, while halving them increases it by 8%.

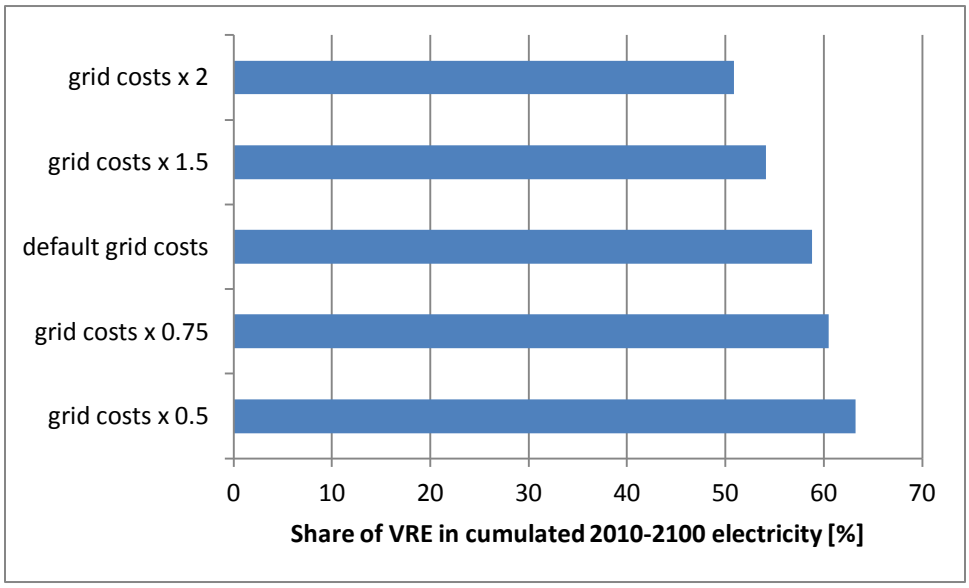


**Figure 16 : Impact of varying the VRE-dependent grid cost markups on the total VRE deployment, here measured by the share of VRE in cumulated 2010-2100 electricity.**